

1 **Title Page**

2

3 **Authors:** Samuel W. Rosenbaum¹, Samuel A. May¹, Kyle R. Shedd², Curry J. Cunningham¹,
4 Randy L. Peterson³, Brian W. Elliot⁴, Megan V. McPhee¹

5

6 **Contact Information:** sam.rosenbaum@umontana.edu, samay3@alaska.edu,
7 kyle.shedd@alaska.gov, cjcunningham@alaska.edu, randy.peterson@alaska.gov,
8 brian.elliott1@alaska.gov, mvmcphee@alaska.edu

9

10 **Affiliation Information:** ¹College of Fisheries and Ocean Sciences, University of Alaska
11 Fairbanks, Juneau, Alaska; ²Alaska Department of Fish & Game, Anchorage, Alaska; ³Alaska
12 Department of Fish & Game, Douglas, Alaska; ⁴Alaska Department of Fish & Game, Haines,
13 Alaska

14

15 **Corresponding Author:** sam.rosenbaum@umontana.edu

16

17 **Running Title:** Reliability of trans-generational genetic mark-recapture (tGMR) for enumerating
18 Pacific salmon

19

20 **Abstract:** As Pacific salmon (*Oncorhynchus* spp.) decline across much of their range, it is
21 imperative to further develop minimally invasive tools to quantify population abundance. One
22 such advancement, trans-generational genetic mark-recapture (tGMR), uses parentage analysis to
23 estimate the size of wild populations. Our study examined the precision and accuracy of tGMR

24 through a comparison to a traditional mark-recapture estimate for Chilkat River Chinook salmon
25 (*O. tshawytscha*) in Southeast Alaska. We examined how adult sampling location and timing
26 impact tGMR by comparing estimates derived using samples collected in the lower river
27 mainstem to those using samples obtained in upriver spawning tributaries. Results indicated that
28 tGMR estimates using a representative sample of mainstem adults were most concordant with,
29 and 3% more precise than, the traditional mark-recapture estimate for this stock. Importantly, the
30 timing and location of adult sampling were found to impact abundance estimates, depending on
31 what proportion of the population dies or moves to unsampled areas between downriver and
32 upriver sampling events. Additionally, we identified potential sources of bias in tGMR arising
33 from violations of key assumptions using a novel individual-based modeling framework,
34 parameterized with empirical values from the Chilkat River. Simulations demonstrated that
35 increased reproductive success and sampling selectivity of older, larger individuals, introduced
36 negative bias into tGMR estimates. Our individual-based model offers a customizable and
37 accessible method to identify and quantify these biases in tGMR applications
38 (https://github.com/swrosenbaum/tGMR_simulations). We underscore the critical role of system-
39 specific sampling design considerations in ensuring the precision and accuracy of tGMR
40 projects. This study validates tGMR as a potentially useful tool for improved population
41 enumeration in semelparous species.

42

43 **Keywords:** Pacific salmon, abundance estimation, trans-generational genetic mark-recapture,
44 close-kin mark-recapture, individual-based model, dropout

45

46 **Acknowledgements:** We thank the ADF&G field crew in Haines, AK for collecting tissue
47 samples for this project. Similarly, we thank staff from the ADF&G Gene Conservation
48 Laboratory for DNA extraction and genotyping, specifically Zac Grauvogel, Zach Pechacek, Jodi
49 Estrada, and Heather Hoyt. Funding for genotyping and pedigree analysis was provided by the
50 Pacific Salmon Treaty Chinook Letter of Agreement Funding under award NA20NMF4380182
51 from the National Oceanic and Atmospheric Administration (NOAA), U.S. Department of
52 Commerce. Funding for a graduate student was partially financed by the Alaska Sustainable
53 Salmon Fund (Project Number 54018) under award NA20NMF4380259 from NOAA,
54 administered by the Alaska Department of Fish and Game. The statements, findings,
55 conclusions, and recommendations are those of the author(s) and do not necessarily reflect the
56 views of the U.S. Department of Commerce, National Oceanic and Atmospheric Administration,
57 or the Alaska Department of Fish and Game.

58

59 **Ethics:** This manuscript has not been submitted elsewhere and all research meets the ethical
60 guidelines of the study country.

61

62 **Conflict of Interest Statement:** The authors declare no conflict of interest.

63

64 **Author Contributions:** S. Rosenbaum performed analyses, co-led study design of the
65 individual-based modeling framework, and wrote the paper. S. May co-led study design of the
66 individual-based modeling framework, aided in analyses, and edited the paper. K. Shedd co-led
67 study design of the Chilkat River tGMR experiment, obtained funding, coordinated laboratory
68 work, genotyping, and pedigree reconstruction, and edited the paper. C. Cunningham co-led

69 study design of the individual-based modeling framework, aided in analyses, and edited the
70 paper. R. Peterson co-led study design of the Chilkat River tGMR experiment, obtained funding,
71 and edited the paper. B. Elliot co-led study design of the Chilkat River tGMR experiment, led
72 field collections, and provided maps of the study system. M. McPhee aided in study design,
73 obtained funding, and edited the paper.

74

75 **Introduction**

76 Anthropogenic pressures are driving declines in Pacific salmon (*Oncorhynchus* spp.)
77 abundance across much of their range (Beamish, 2022; Riddell et al., 2022), negatively
78 impacting salmon-reliant ecosystems, cultures, and economies. Efforts to restore Pacific salmon
79 populations require accurate and precise estimates of key demographic quantities, such as the
80 number of mature adults returning to spawn, commonly referred to as “escapement”. Salmon
81 fisheries are often managed to meet escapement goals, determined by state and federal agencies
82 (Clark et al., 2006). Improving the reliability and efficiency of salmon escapement enumeration
83 methods will aid sustainable management of Pacific salmon populations.

84 Mark-recapture experiments, which are commonly used for fisheries management
85 (Adkison, 2022), traditionally rely on physically tagging individuals for population abundance
86 estimation (Pradel, 1996). While these methods can provide reliable abundance estimates under
87 specific conditions, meeting necessary assumptions is challenging, often resulting in reduced
88 precision of abundance estimates (Roff, 1973). Notably, physical tags may be lost or affect
89 individual behavior, leading to potentially misleading estimates (Seber & Felton, 1981). Failure
90 to identify recaptured individuals can lead to an over-estimation of abundance, further imperiling

91 declining populations by enabling over-harvest. Innovations in tagging methodology are
92 therefore beneficial for remedying these deficiencies.

93 Recent years have seen a growing interest in molecular applications of the mark-
94 recapture framework, broadly known as close-kin mark-recapture (CKMR) (Bravington et al.,
95 2016). CKMR uses multi-locus genotypes to mark individuals, and subsequent sampling the
96 close kin of marked individuals are treated as “recapture” events. Because the CKMR framework
97 does not require physical tags or repeated sampling of individuals, it reduces sampling
98 invasiveness while increasing efficiency. CKMR estimators frequently produce population
99 estimates with higher precision than conventional abundance monitoring techniques (e.g.,
100 traditional mark-recapture and redd count expansion) for a broad range of iteroparous marine
101 (Bravington et al., 2016; Hillary et al., 2018; Patterson et al., 2022; Delaval et al., 2023) and
102 freshwater (Ruzzante et al., 2019; Marcy-Quay et al., 2020; Prystupa et al., 2021; Wacker et al.,
103 2021) fishes.

104 Trans-generational genetic mark-recapture (tGMR) is a specific application of CKMR
105 designed for enumerating semelparous species, such as Pacific salmon. Within the tGMR
106 framework, the initial sampling event comprises genetic sampling of spawning adults and the
107 second sampling event involves genetic sampling of potential offspring (Rawding et al., 2014). A
108 distinct advantage of tGMR lies in its ability to “tag” numerous offspring by genotyping only a
109 comparatively small number of adults, thereby increasing precision through a greater number of
110 recaptures. However, robust inference from mark-recapture estimates is contingent upon meeting
111 or accounting for model assumptions (Seber, 1982). While tGMR and traditional mark-recapture
112 assumptions are nearly identical (Peterson et al., 2023), methods for evaluating tGMR
113 assumptions are not well developed given that the availability of offspring for recapture is

114 mediated by the reproductive success of adults. Specifically, the assumptions of (1) equal
115 probability of capture within the first sampling event and (2) a closed population between
116 sampling events may be violated when enumerating Pacific salmon (Rawding et al., 2014; Small
117 et al., 2020), because sampling selectivity of adults may covary with reproductive success.

118 tGMR estimates could be biased if there are conditions that jointly influence the
119 probability of certain adults and their offspring being captured (i.e., violating assumption 1).

120 There are several aspects of Pacific salmon life history and common sampling techniques that
121 could lead to these biases. For example, age, body size, and sampling selectivity are correlated in
122 most salmonids and are often important determinants of reproductive success (reviewed in Koch
123 & Narum, 2021). Thus, it is important to evaluate potential biases in tGMR estimates by
124 examining the influence of age and size on variability in reproductive success and sampling
125 selectivity.

126 Another factor complicating tGMR estimation is the biological complexity of freshwater
127 migration and the potential for loss of adults between sampling events, violating assumption 2.
128 Chinook salmon handled in mark-recapture or telemetry studies may enter rivers but later move
129 back into saltwater habitat, becoming vulnerable to marine sources of mortality including harvest
130 (Sethi & Tanner, 2014). Additionally, prespawn mortality of adult salmon can occur within
131 freshwater habitats (Bowerman et al., 2016), and mature adults can migrate to unsampled
132 spawning habitat within a watershed. Past tGMR studies were limited to collecting adult tissue
133 samples (“marks”) from carcasses only encountered in upstream tributary habitat (Rawding et
134 al., 2014; Whitmore 2016; Small et al., 2020). However, by sampling mature adults both initially
135 in the lower mainstem river and later in the upriver tributary habitats, separate tGMR estimates

136 can be calculated, potentially allowing one to estimate rates of loss between mainstem and
137 spawning reaches.

138 Individual-based models are a powerful tool for examining population dynamics of
139 Pacific salmon (Reed et al., 2011; Lin et al., 2017; Yeakel et al., 2018; May et al., 2023).
140 Simulation models parameterized with empirical data have proved particularly useful for
141 exploring emergent properties of life-history dynamics that are difficult to measure in natural
142 systems (Berdahl et al., 2018). Recent modeling work has broadly highlighted the importance of
143 accounting for variation in life-history traits and experimental design when implementing
144 CKMR (Waples & Feutry, 2022). Developing a flexible and user-friendly simulation framework
145 to quantify bias specifically associated with violations of tGMR assumptions could help guide
146 future tGMR applications.

147 The present study aimed to evaluate the suitability of tGMR methods for escapement
148 estimation by exploring how differences in adult sampling can lead to bias. To meet this goal, we
149 conducted a case study on Chinook salmon (*O. tshawytscha*) returning to the Chilkat River,
150 Alaska in 2020 with the following objectives: 1) compare abundance estimates and their
151 precision derived from tGMR with traditional mark-recapture; 2) investigate the effect of
152 variation in reproductive success and adult sampling selectivity on tGMR abundance estimates
153 (assumption 1 violations); and 3) explore the effect of adult sampling location and timing on
154 tGMR abundance estimates (assumption 2 violations). To achieve these objectives, we calculated
155 tGMR abundance estimates using adults sampled in both the lower mainstem river during initial
156 freshwater migration and later in upriver tributaries during spawning. We then designed an
157 individual-based simulation framework for examining sources of bias in tGMR applications,
158 which can be used in other semelparous species and systems to evaluate the impact of

159 assumption violations (https://github.com/swrosenbaum/tGMR_simulations). tGMR may
160 provide a more efficient and less invasive tool to enumerate adult salmon populations and could
161 offer increased precision when compared with traditional mark-recapture methods. By
162 addressing key knowledge gaps, we aimed to assess the reliability of extending tGMR across the
163 range of semelparous salmon for improved enumeration of these iconic species.

164 **Methods**

165 **Study System**

166 In 2020, a tGMR experiment was conducted on Chinook salmon returning to the Chilkat
167 River, located near Haines, AK (Figure 1A). The Chilkat River is the third largest producer of
168 Chinook salmon in Southeast Alaska (McPherson et al., 2003) and is an exploitation rate and
169 escapement indicator stock monitored by the Pacific Salmon Commission under the Pacific
170 Salmon Treaty (Chinook Technical Committee 2021). The Chilkat River Chinook salmon stock
171 is critical to subsistence fishers in the region, who catch as much as 17% of the total Chilkat
172 River Chinook salmon harvest in some years. The Chilkat River Chinook salmon stock only
173 reached its escapement goal once during 2012–2017, resulting in its designation as a “stock of
174 management concern” by the Alaska Department of Fish and Game (ADF&G) in 2017 (Lum &
175 Fair, 2018). Following this designation, the estimated 2018 escapement was the lowest in the
176 history of the time series. Due to this population’s decline and subsequent ADF&G management
177 designation, the subsistence fishery for Chilkat River Chinook salmon has been closed since
178 2017 (Elliott & Peterson, 2022). In an era of declining salmon populations and decreasing
179 budgets for management agencies, fewer resources are available for monitoring activities, and
180 managers may implement precautionary approaches by further reducing harvest.

181 The Chilkat River Chinook salmon stock is currently monitored through a long-term
182 traditional mark-recapture project occurring annually since 1991 (Ericksen & McPherson 2004),
183 making it an excellent system in which to evaluate tGMR methods. The existing traditional
184 mark-recapture project utilizes multiple gears to capture fish in both the lower mainstem river
185 during freshwater migration (adult event 1; fishwheels and drift gillnets) and upriver tributary
186 sampling on spawning grounds (adult event 2; rod and reel, seining, and/or carcass sampling).
187 The combination of sampling gear and their associated biases are discussed below and have been
188 implemented by ADF&G to estimate the abundance of large adult Chinook salmon \geq age 4 (1.2
189 in European notation, Koo 1955). The successful application of tGMR for estimating escapement
190 of Chilkat River Chinook salmon may allow extension of this method to other Alaskan salmon
191 stocks that currently lack intensive monitoring programs, for more precise escapement
192 estimation.

193 **Sampling**

194 Elliott & Peterson (2022) estimated the abundance of returning Chinook salmon (\geq age
195 4; 1.2 in European notation) entering the Chilkat River in 2020 using a traditional two-sample
196 mark-recapture study for a closed population (Seber, 1982). Returning adult Chinook salmon
197 were captured during freshwater migration in June and July using fishwheels and drift gillnets (7
198 $\frac{1}{2}$ inch mesh) during event 1 in the lower mainstem of the Chilkat River and marked with Floy
199 T-bar tags (Figure 1B). Use of fishwheels (selective for smaller, younger fish) and drift gillnets
200 (selective for larger, older fish) helped ensure a representative sample of all adult size and age
201 classes was collected (Elliott, 2022). Event 2 sampling occurred during August in the three major
202 spawning tributaries of the upper Chilkat River using rod and reel, dip nets, short tangle nets,
203 beach seines, and carcass surveys. Potential biases and sources of errors were evaluated using the

204 methods outlined in Elliott (2022). Abundance of adult Chinook salmon (excluding age-3 males,
205 1.1, or “jacks”) was estimated using Chapman’s modification of Petersen’s mark-recapture
206 method (Chapman, 1951). Jacks were excluded from the traditional estimate as the capture rate
207 for these younger, smaller individuals on the spawning grounds during the adult event 2
208 sampling was insufficient for robust estimation of this age-class (proportion sampled = 0.01). We
209 used the results of this traditional mark-recapture effort to compare the precision and agreement
210 of our tGMR case study detailed below.

211 Tissue samples were collected from the adults sampled as part of the traditional mark-
212 recapture study (adult events 1 and 2; Elliott 2022). Both events were treated as ‘marks’ for the
213 tGMR method. Pelvic fin tissue samples were collected and dried on Whatman paper to preserve
214 DNA. Additional metadata were recorded for each individual, including body length (mid eye to
215 tail fork), sex, sample date, sample location, and age from scale samples (Peterson et al., 2023).

216 Juvenile tissue samples were collected in the fall of 2021 from fall parr rearing in the
217 Chilkat River using the methods described in Elliott & Peterson (2022). These samples represent
218 our second sampling event in the tGMR experiment (hereafter ‘captures’). Parr were sampled
219 using a stratified systematic sampling design, with samples collected continuously throughout
220 September and October, across the mainstem and two of the three primary spawning tributaries
221 of the Chilkat River using baited minnow traps (Figure 1C). As an alternative to fin clipping parr
222 Chinook salmon, tissue samples were collected non-lethally using OmniSwabs (Qiagen,
223 Whatman FTA), which were used to collect DNA from external fish mucus in a minimally
224 invasive manner. OmniSwabs were preserved dry in 2ml cryovials filled with silica desiccant
225 beads to preserve DNA. We recorded additional metadata for each individual, including body
226 length (fork length), sample date, and sample location.

227 **Molecular Protocol**

228 Genetic analysis was conducted at the ADF&G Gene Conservation Laboratory in
229 Anchorage, AK. Following the methods outlined in Peterson et al. (2023), we extracted genomic
230 DNA from adult pelvic fin samples and parr OmniSwabs swabs separately using NucleoSpin®
231 Tissue Kits (Macherey-Nagel). We genotyped each sample using two different methods: 1)
232 Genotyping-in-Thousands by sequencing (GT-seq; Campbell et al., 2015) for 299 single
233 nucleotide polymorphism (SNP) genetic markers in the 299 SNP v3.0 GT-seq panel developed
234 by the Columbia River Inter-tribal Fish Commission Hagerman Genetics Laboratory (Hess et al.,
235 2014; Appendix S1), and 2) polymerase chain reaction (PCR) fragment analysis for 5 multi-
236 plexed microsatellite loci from the Genetic Analysis of Pacific Salmon (GAPS) panel (Seeb et
237 al., 2007; Moran et al., 2013; Appendix S1).

238 GT-seq SNP libraries were sequenced on an Illumina NextSeq 500 with single-end 150
239 base-pair reads. Individual genotypes were called using *GTscore*
240 (<https://github.com/gjmckinney/GTscore>), a custom GT-seq genotype-calling pipeline that uses
241 sequence matching to quantify allelic count and ratios for each marker to infer genotype
242 (McKinney et al., 2020). We then imported our genotype data into the ADF&G database LOKI.
243 SNPs in the GT-seq panel were removed from use in downstream analyses based on their
244 performance in the Southeast Alaska Chinook salmon genetic baseline (Shedd & Gilk-Baumer
245 2021). Briefly, Shedd & Gilk-Baumer (2021) excluded loci if: 1) visual examination of allelic
246 ratio plots indicated non-singleton allelic ratios (i.e., diverged duplicate or duplicated loci), 2)
247 loci failed to conform to Hardy-Weinberg expectations (HWE), and 3) if pairs of loci were in
248 linkage disequilibrium (LD).

249 Five of thirteen microsatellite loci from the GAPS panel (*Omm1080*, *Ots213*, *Ots201b*,
250 *Ssa408uos*, and *Ots9*) were amplified in a single, multiplexed PCR reaction following methods
251 described in Seeb et al. (2007). PCR products were visualized using a 3730 capillary DNA
252 analyzer (Applied Biosystems). Genotypes were scored manually with GeneMapper software
253 (version 4.0, Applied Biosystems) and then imported into the ADF&G database LOKI.

254 To identify laboratory errors and quantify the genotyping error rate for use in
255 downstream parentage analyses, 8% of sampled individuals were re-extracted and assayed for
256 the same set of markers described above. The discrepancy rate, which reflects DNA extraction,
257 assay plate, and genotyping errors, was calculated as the number of conflicting genotypes
258 divided by the total number of genotypes compared. The discrepancy rate was then divided by
259 two to give the genotyping error rate.

260 Following procedures described in Shedd et al. (2022), we adapted custom scripts
261 (<https://github.com/krshedd/GCL-R-Scripts>) to further filter our genotype data using the
262 programming language R (R Core Team 2018). These scripts removed individuals missing 20%
263 or more of their genotypes, duplicate individuals identified as sharing at least 95% of their
264 genotypes, and potentially contaminated individuals identified by excessively heterozygous SNP
265 genotypes (defined by a cutoff of 1.5 times the interquartile range). These steps were intended to
266 reduce quality issues resulting from low-grade DNA, duplicate sampling, and contamination.

267 **tGMR Abundance Estimation**

268 To determine kinship relationships among adults and juveniles, the parentage analysis
269 program COLONY was used to reconstruct a one-generation pedigree (version 2.0.6.8) (Wang &
270 Santure, 2009). COLONY is a full probability pedigree reconstruction software that uses
271 maximum likelihood to reconstruct full- and half-sibling family groups among juveniles and

272 assigns parents to family groups. Additionally, COLONY infers genotypes of unsampled parents
273 through information of sibling relationships among juveniles. Reconstructing unsampled parental
274 genotypes allows for putative identification of the total number of reproductively successful
275 adults, both sampled and unsampled. Simulations indicated a large number of polymorphic
276 markers (several hundred) are necessary for valid inference of unsampled parents when using
277 prior versions of COLONY (version 2.0.6.1) (Whitmore 2016). These inferred parental
278 quantities are necessary for the hypergeometric implementation of tGMR (described below). We
279 decided to not use sex data as an input to COLONY as non-lethal identification of sex in adult
280 salmon is error prone (Chapell 2014), especially in the lower river mainstem, and the genotyping
281 panel used in these analyses lacks a reliable sex marker. We assumed male and female polygamy
282 without inbreeding. All COLONY input parameters are provided in Table S1. To assess the
283 potential influence of *en route* loss of adults (from here on referred to as “dropout”) on tGMR
284 abundance estimates, we ran COLONY on three separate datasets to identify pedigree
285 relationships between: 1) all adults and all juveniles; 2) adults sampled in the lower mainstem
286 river and all juveniles; and 3) adults sampled in the upriver tributaries and all juveniles. Prior to
287 each of the three COLONY runs, we identified and removed any duplicate individuals (including
288 adult recaptures when analyzing all adults) (Table S2).

289 Abundance estimates were derived from pedigree outputs from COLONY using both the
290 binomial and hypergeometric tGMR models described by Rawding et al. (2014) and later
291 adjusted by Small et al. (2020) and Peterson et al. (2023). Briefly, the binomial estimator allows
292 sampling with replacement and estimates the adult population size (N_{bin}) from the number of
293 adults genotyped (marks, M), the number of parr genotyped multiplied by two (captures, C), and
294 the number of POPs (recaptures, R). The number of sampled parr is multiplied by two because

295 the parental genotype is the mark, and because juveniles carry genotypes from dams and sires,
 296 they have two opportunities to recapture marks. Under this sampling-with-replacement
 297 framework, all juvenile data are incorporated into the estimator regardless of whether multiple
 298 juveniles share one or both parents (resampling). In other words, siblings from the same parent
 299 are counted as separate recaptures and represent unique POPs. On the other hand, the
 300 hypergeometric estimator implements sampling without replacement, where only the first
 301 ‘sampling’ of a parent by a genotyped parr is considered. This estimator relies on the number of
 302 unsampled parents inferred by COLONY. In this case, M is still the number of adults genotyped,
 303 but C is the number of unique parents inferred from offspring kinship relationships, both
 304 sampled and unsampled, and R is the number of unique sampled parents assigned to at least one
 305 offspring.

306 Escapement estimated using Bailey’s modified binomial model (Small et al., 2020) was:

307

$$308 \quad N_{bin} = \frac{M(C+1)}{(R+1)} \quad (\text{Eq. 1})$$

309

310 Variance was estimated using Bailey's (1951) approximation:

311

$$312 \quad \text{var} (N_{bin}) = \frac{M^2(C+1)(C-R)}{(R+1)^2(R+2)} \quad (\text{Eq. 2})$$

313

314 Escapement estimated using Chapman’s modified hypergeometric model was:

315

$$316 \quad N_{hyp} = \frac{(M+1)(C+1)}{(R+1)} - 1 \quad (\text{Eq. 3})$$

317

318 Variance of N_{hyp} was estimated as:

319

$$320 \quad \text{var}(N_{hyp}) = \frac{(M+1)(C+1)(M-C)(C-R)}{(R+1)^2(R+2)} \quad (\text{Eq. 4})$$

321

322 Confidence intervals for both N_{bin} and N_{hyp} were calculated using a normal approximation as the
323 number of recaptures was expected to be large.

324 **Simulations to Quantify Bias from Assumption Violations**

325 **Individual-Based Model Overview**

326 To examine the accuracy and precision of tGMR estimation under varying demographic
327 and sampling scenarios we implemented a paired simulation-estimation approach. Specifically,
328 we constructed an individual-based simulation model of a single semelparous salmonid
329 population across one generation, in which adult salmon were sampled as they returned to
330 spawning grounds (marks) and later their juvenile offspring were sampled (captures; Figure 2).
331 This model was used to examine the effect of two variables on tGMR abundance estimation: (1)
332 age-specific differences in adult reproductive success (\mathbf{P}_{RS}) and (2) age-specific differences in
333 adult sampling selectivity ($\mathbf{P}_{\text{sampling}}$), which were both vectors of age-specific probabilities input
334 as initial parameters. Age-specific differences in reproductive success were defined as the
335 relative probability of individuals of a certain age producing at least one offspring when
336 compared to a different age class. Age-specific differences in adult sampling selectivity were
337 defined as the relative probability of individuals of a certain age class being sampled during
338 event 1 of tGMR sampling as they returned to spawning grounds. These demographic parameters
339 are expected to bias tGMR estimates through their combined effect on the number of recaptures
340 identified through parentage analysis (Waples & Feutry, 2022). We parameterized the model

341 with values from our empirical tGMR case study on Chinook salmon from the Chilkat River to
342 quantify the direction and magnitude of bias in tGMR estimates arising from differences in age-
343 specific reproductive success and non-uniform event 1 (adult) sampling selectivity at age.

344 **Model Initialization**

345 We initialized the simulation with a known number of adults (N_{adults}) and offspring
346 ($N_{\text{offspring}}$) parameterized based on our case study system (Table 1). Each adult was assigned
347 three parameter values: (1) age, (2) probability of reproductive success, and (3) probability of
348 being sampled conditional on the assumed selectivity of the event 1 adult sampling process.
349 First, ages (**Ages**) were assigned to individuals using a weighted draw from a vector of ages (3,
350 4, 5, or 6 years old) proportional to the observed average age composition of Chilkat River adult
351 Chinook salmon across the mainstem 2020 sampling effort (\mathbf{P}_{age}). This initial input parameter
352 determined the age structure of the returning adult population encountered during event 1
353 sampling. Second, reproductive success probabilities for individual adults were dependent on
354 their age and were assigned from a constant vector of age-specific reproductive success
355 probabilities (\mathbf{P}_{RS}), such that all individuals of a given age had the same probability of having
356 offspring. There was no additional random variation in age-specific reproductive success values,
357 although such variation could be incorporated in future model applications. \mathbf{P}_{RS} was estimated
358 from empirical data from both mainstem and tributary adults as a vector of age-specific mean
359 reproductive success values, where reproductive success was a Bernoulli variable (zero offspring
360 or >0 offspring). Third, individual sampling probabilities were also dependent on age values and
361 assigned from a vector of age-specific sampling selectivity values ($\mathbf{P}_{\text{sampling}}$). A subset of parents
362 in the simulated spawning population were sampled (n_{adults}) as they returned to hypothetical natal
363 rivers, conditional on their age-specific sampling probability. Parents were assigned to offspring

364 using a weighted draw of n_{adults} from all possible parents in the population (N_{adults}). We did not
365 parameterize these values differently by sex, but this could be implemented in future
366 applications.

367 The value $N_{\text{offspring}}$ determined the census size of parr in the next generation, which was
368 held constant across simulations in this study. Offspring were each assigned one parent, using
369 methods adapted from *TheWeight* (Waples, 2022) by using a random draw from all possible
370 parents, weighted by P_{RS} values of parents. Then, a proportion of offspring were randomly
371 sampled from all offspring in the population, representing juvenile sampling. The number of
372 offspring sampled was also set as an initial input parameter ($n_{\text{offspring}}$). We performed a
373 hypothetical molecular pedigree reconstruction from sampled parents and offspring, assuming
374 perfect parentage assignment. For each unique set of input parameters, the simulation was re-run
375 for 1,000 iterations to quantify uncertainty.

376 **Model Outputs**

377 Model outputs comprised an incomplete pedigree containing sampled offspring and their
378 assigned parent, if sampled, in addition to the ages of the known parents. These data were then
379 used to quantify key population abundance statistics, such as the number of POPs and a tGMR
380 estimate analogous to a single-sex binomial estimate. Mean tGMR estimates (Equation 5) and
381 the range of abundances predicted by 95% of the simulations were quantified across 1,000
382 iterations per simulation. By not accounting for sex, our model produces tGMR estimates that do
383 not directly follow the currently established binomial or hypergeometric tGMR frameworks. Our
384 simplified approach assumed equal sex ratios and no variability in reproductive success or
385 sampling selectivity between the sexes.

386

$$387 \quad \text{Averaged Model Estimate} = \frac{(\text{mean}(n_{\text{adult}}) * (\text{mean}(n_{\text{offspring}})) + 1)}{(\text{mean}(POPs) + 1)} \quad (\text{Eq. 5})$$

388 **Model Parameterization**

389 \mathbf{P}_{RS} was calculated from our empirical Chilkat River case study by identifying the mean
 390 reproductive success for each age-class. We used 434 ages from scale samples collected from
 391 both the lower river and the upstream tributaries from the case study system, and we used only
 392 these 434 individuals with known ages for reproductive success analysis (Figure S1).

393 $\mathbf{P}_{\text{sampling}}$ was also calculated from the case study data using the 434 adults with known
 394 ages from scale age analysis. We first estimated the “true” age structure of the population using
 395 adults sampled from the lower mainstem. As discussed previously, adults sampled in the lower
 396 mainstem river are thought to provide the most accurate representation of the population’s age
 397 structure due to the use of fishwheels and gillnets with differing selectivity. Next, the relative
 398 selectivity for the upriver tributary sampling event was estimated by calculating the age structure
 399 within tributary adults by dividing the number of adults of a given age within the tributary by the
 400 “true” age structure calculated from the mainstem adults. Finally, we standardized selectivity
 401 within the tributary by dividing the relative age structure for the tributary sampling event by the
 402 sum of the relative age structure for the tributary sampling event.

403 **Asymptotic Reproductive Success and Sampling Selectivity (Violating Assumption 1)**

404 To examine how age-specific differences in reproductive success and sampling
 405 selectivity influence the accuracy and precision of tGMR estimation, we parameterized our
 406 model with a range of values for the age-specific vectors \mathbf{P}_{RS} and $\mathbf{P}_{\text{sampling}}$. To explore a range of
 407 possible scenarios in which reproductive success or selectivity of adult sampling varied with age,
 408 we generated values for these parameters from a logistic function (Equation 6), where the slope

409 of the relationship between reproductive success or sampling selectivity and age was determined
 410 by a slope variable (δ), and the a_{50} parameter was fixed at the mean of observed ages (4.5).

$$411 \quad \mathbf{P}_{RS} \text{ or } \mathbf{P}_{\text{sampling}} \text{ for a given } \delta \text{ scenario} = 1 + e^{(-1 * \delta(\text{age} - a_{50}))^{-1}} \quad (\text{Eq. 6})$$

412 We scaled δ continuously across the values -3 to 3, which encompasses a range of plausible life
 413 history patterns of these traits for many salmonids and drew $\mathbf{P}_{\text{sampling}}$ and \mathbf{P}_{RS} values across the
 414 scope of δ values. For each δ value, the corresponding \mathbf{P}_{RS} and $\mathbf{P}_{\text{sampling}}$ vectors were used as
 415 simulation inputs while holding all other input parameters constant. \mathbf{P}_{RS} and $\mathbf{P}_{\text{sampling}}$ were
 416 examined separately, varying only one parameter at a time while holding the other constant at
 417 values of 0.07, 0.17, 0.28, 0.38 for \mathbf{P}_{RS} and 0.10, 0.40, 0.70, or 0.10 for $\mathbf{P}_{\text{sampling}}$. The constant
 418 values reflect estimated quantities from the combined mainstem and tributary Chilkat River adult
 419 sampling events. Each δ scenario was evaluated across 1,000 model iterations for each set of \mathbf{P}_{RS}
 420 and $\mathbf{P}_{\text{sampling}}$ values separately, with among-iteration differences arising from random variation in
 421 which: (1) individual adults were captured during event 1; (2) individual adults produced
 422 offspring; and (3) individual offspring were sampled during event 2. The model outputs from
 423 these iterations quantified the range of bias in tGMR estimates resulting from variation in
 424 reproductive success-at-age and selectivity-at-age predictions. Bias was calculated as the
 425 difference between the averaged point estimate across the 1,000 iterations and the “true” input
 426 $N_{c_{adults}}$ value, divided by $N_{c_{adults}}$ (Equation 7).

$$427 \quad \text{Bias} = \frac{(\text{Averaged Model Estimate} - N_{c_{adults}})}{N_{c_{adults}}} \quad (\text{Eq. 7})$$

428 **Comparison of Mainstem vs Tributary tGMR Estimates (Violating Assumption 2)**

429 To examine how adult sampling location and timing of capture may impact tGMR
 430 estimates, we compared hypergeometric tGMR estimates inferred based on three adult Chinook
 431 collections: 1) lower mainstem Chilkat River adults sampled in June and July; 2) upriver

432 tributary adults sampled in August; and 3) adults from both sampling events, combined. We used
433 separately reconstructed pedigrees for these three collections. The resulting hypergeometric
434 tGMR estimates and their confidence intervals (calculated using a normal approximation) were
435 then compared. Hypergeometric estimates were used as opposed to binomial estimates, because
436 the hypergeometric model is more robust to violations of assuming an equal probability of
437 capture during the adult sampling event (Rawding et al., 2014; Small et al., 2020). The
438 hypergeometric model is generally more robust in salmonid systems, as the sampling without
439 replacement framework buffers against heterogeneity in reproductive success that may lead to
440 violations of this core assumption (Small et al., 2020).

441 Differences in tGMR estimates between lower mainstem and upriver tributary samples
442 could result from violations of assumptions in either estimate or the loss of adults from the
443 population during freshwater migration. We defined dropout as the number of adults that may be
444 sampled in the lower mainstem river but are subsequently unable to be sampled in the upriver
445 tributaries for any reason that would violate the assumption of a closed population, such as
446 movement out of the study area or accidental capture mortality. The potential influence of adult
447 dropout on tGMR abundance estimation was examined with our individual-based modeling
448 framework, which assumes that assumptions are otherwise met for both estimates. Nine
449 simulation scenarios were implemented with varying rates of dropout from 0% to 40%, in
450 increments of 5%, based on a range thought to encompass a plausible set of values likely to
451 occur in Alaska watersheds (Richards et al., 2017). Input P_{sampling} values for the lower mainstem
452 and upriver tributary simulation scenarios were re-calculated separately for each traditional adult
453 sampling event/gear type in the same manner described in the “Model Parameterization” section.
454 These re-calculations were performed to better reflect the selectivity conditions occurring during

455 these discrete sampling periods (Table 2; Figure S2), improving our ability to compare simulated
456 and empirical results. Model outputs (e.g., mean tGMR estimates) were then compared to the
457 empirical hypergeometric mainstem and tributary tGMR estimates.

458 **Results**

459 **Genotyping**

460 The average genotyping success rate across all adult fish using GT-seq was 99.70%. The
461 average genotyping success rate across all juveniles using GT-seq was 98.23%. There were 41 of
462 the 641 adults and 7 of the 700 parr that had contamination scores deemed too high to allow for
463 accurate microsatellite genotyping. The entire multiplex of five microsatellite loci were retained
464 for analyses, however 26 of the 299 SNPs were dropped due to sequencing issues (non-singleton
465 allelic ratios), 11 SNPs were dropped due to violations of HWE, and 8 SNPs were dropped due
466 to LD with other SNPs (Shedd & Gilk-Baumer, 2021). Our final genotyping panel consisted of
467 259 loci (254 SNPs and 5 microsatellites).

468 We removed 10 individuals from analyses that were missing greater than or equal to 20%
469 of their genotypes (Dann et al. 2012). Furthermore, we removed 20 duplicated fish from our
470 study. Most of these duplicates were recaptured adults that had been sampled during both adult
471 sampling occasions (mainstem and tributary projects). We removed 46 outliers that fell outside
472 the 1.5 interquartile range of individual heterozygosity. These individuals were likely
473 excessively heterozygous because of contamination. The final dataset considered in all
474 subsequent analyses (Table S2) included 583 adults (sample locations described in Table S3) and
475 682 juvenile Chinook salmon (sample locations described in Table S4).

476 **Traditional and tGMR Abundance Estimates**

477 Elliott & Peterson (2022) estimated the 2020 escapement of non-jack Chilkat River
478 Chinook salmon (\geq age 4) to be 3,769 fish (95% CI: 2,726 – 4,812; Figure 3; Table 3).

479 COLONY identified 237 POPs, 148 unique sampled parents, and 745 total inferred
480 parents from within the complete sample of 583 adults and 682 juvenile Chinook salmon. The
481 583 adult genotypes were considered the marks in both the binomial (with replacement) and
482 hypergeometric (without replacement) estimators (Table 3). The captures in the binomial model
483 were the 682 juveniles genotyped multiplied by two (each offspring has two potential parents),
484 and the recaptures in the binomial model were the 237 POPs. The 745 unique parents inferred
485 from the offspring using COLONY were considered the captures for the hypergeometric model,
486 and the 148 unique sampled parents assigned to the offspring were the recaptures in the
487 hypergeometric model. The escapement estimate calculated with the binomial model using all
488 sampled adults was 3,344 fish (95% CI: 2,958 – 3,729). Using the hypergeometric model while
489 including all adults, we estimated escapement to be 2,923 spawners (95% CI: 2,562 – 3,284;
490 Figure 3; Table 3).

491 **Simulations to Quantify Bias from Assumption Violations**

492 **Model Parameterization**

493 The mean probability of reproductive success at a given age (P_{RS}) values were 0.07 for
494 age-3 adults, 0.17 for age-4 adults, 0.28 for age-5 adults, and 0.38 for age-6 adults (Figure S1).
495 The calculated age structures and selectivity for each adult sampling event are presented in Table
496 2 and Figure S2.

497 **Asymptotic Reproductive Success (Violating Assumption 1)**

498 We investigated how variation in age-specific reproductive success influenced the
499 magnitude and direction of bias in tGMR abundance estimation. Bias (i.e., the difference
500 between model-estimates and the true adult run size ($N_{c_{adults}}$); Equation 7) increased as
501 reproductive success-at-age decreased. For example, in simulations testing the most extreme
502 decreasing age-specific reproductive success (slope $\delta = -3$), the averaged estimate was positively
503 biased by 33% (Figure 4B). In contrast, bias was close to zero (0.1%) when reproductive success
504 was constant across ages ($\delta = 0$). However, bias became more negative as age-specific
505 reproductive success increased. For example, in the most extreme case of increasing reproductive
506 success-at-age ($\delta = 3$), the averaged point estimate was biased by -10%. Notably, in scenarios
507 with increasing reproductive success-at-age, bias appears to asymptote near -10%. The
508 variability in bias among simulations decreased as δ became increasingly positive (i.e., greater
509 reproductive success at older ages). In contrast, bias did not appear to asymptote with decreasing
510 reproductive success-at-age. The range of bias observed in 95% of simulation iterations for a
511 given δ is represented by the gray shaded area on Figure 4B. Chinook salmon reproductive
512 success is positively associated with age (Koch & Narum, 2021), indicating that the scenarios
513 simulating decreasing age-specific reproductive success ($\delta = -3$, $\delta = -2$, $\delta = -1$) are unlikely to
514 occur in natural systems. However, we include these scenarios as some semelparous fishes may
515 demonstrate this life history pattern and it is therefore useful to fully understand the range of
516 possible effects driven by variable age-specific reproductive success in different systems.

517 **Asymptotic Adult Sampling Selectivity (Violating Assumption 1)**

518 We also investigated how variation in age-specific sampling selectivity influenced the
519 magnitude and direction of bias in tGMR abundance estimation (Figure 4). Bias increased as

520 selectivity-at-age decreased. In simulations with the most extreme decreasing selectivity-at-age (
521 $\delta = -3$), the averaged point estimate was positively biased by 37%. However, bias was nearly
522 zero (0.2%) when selectivity was constant across ages ($\delta = 0$). Bias became more negative as
523 selectivity-at-age increased. Under the most extreme case of increasing selectivity-at-age ($\delta = 3$),
524 the averaged point estimate was biased by -13%. While bias appeared to increase severely and
525 continuously with decreasing selectivity-at-age, under increasing selectivity-at-age, bias
526 appeared to asymptote negatively at -13%. The variability in bias for $\delta = 3$ decreased to nearly
527 zero.

528 **Comparison of Mainstem vs Tributary tGMR Estimates (Violating Assumption 2)**

529 Using 295 returning adult Chinook salmon sampled in the lower mainstem of the Chilkat
530 River in June of 2020 and 682 parr collected in the fall of 2021, COLONY identified 56 unique
531 adult parents assigned to parr offspring and inferred 705 total unique successfully reproducing
532 adults. These quantities produced a hypergeometric tGMR estimate of 3,665 adults (95% CI:
533 2,852 – 4,479) with a CV of 11% (Table 3), based on event 1 adult sampling in the lower
534 mainstem river. Using the 306 adults sampled in upriver spawning tributaries in August of 2020
535 and all 682 sampled parr, COLONY identified 96 unique adult parents assigned to parr offspring
536 and inferred 721 total unique successfully reproducing adults. These quantities produced a
537 hypergeometric tGMR estimate of 2,284 adults (95% CI: 1,936 – 2,632) with a CV of 8%, based
538 on adult event 2 sampling in the spawning tributaries.

539 We evaluated how varying levels of dropout between adult sampling locations (lower
540 river mainstem vs upriver tributary spawning grounds) may influence tGMR estimates. As the
541 percentage of adult dropout increased across simulations, the average estimate based on upriver
542 tributary adult sampling, and the range of abundances predicted by 95% of simulations,

543 decreased (Table S5, Figure 5). For example, at 0% dropout the average abundance estimate was
544 3,283 fish, while at 40% dropout the average abundance estimate was 1,978. Notably, vectors of
545 age-specific sampling selectivity values ($\mathbf{P}_{\text{sampling}}$) used to parameterize the scenarios examining
546 the influence of dropout were calculated from the empirical case study data separately for
547 mainstem $\mathbf{P}_{\text{sampling}} = [0.18, 0.12, 0.60, 0.10]$ and tributary habitats $\mathbf{P}_{\text{sampling}} = [0.01, 0.34, 0.29,$
548 $0.36]$. The simulated differences observed in scenarios in which **Proportion**_{dropout} was held at
549 0% for both lower mainstem river and upriver tributary sampling locations (Figure 6, left panel)
550 is attributable to differences in $\mathbf{P}_{\text{sampling}}$. The difference between these estimates was 144 fish
551 (Figure 6, left panel; calculated from Table S5), which was insufficient to explain the empirically
552 observed difference in abundance estimates between the mainstem and tributary habitats (1,381
553 fish, Figure 6 right panel, calculated from Table 3). The simulation scenario with a 30% dropout
554 rate (Figure 6, middle panel) produced an average estimate (2,281 fish; 95% predicted range:
555 1,855 – 2,706) which aligned well with the empirical hypergeometric tGMR estimator calculated
556 using only tributary adults (2,284 fish; 95% CI: 1,936 – 2,632; Tables 3 and S3). This simulated
557 exploration of varying dropout rates and selectivity differences between adult sampling locations
558 explores one potential mechanism underpinning the differences we observed between our
559 mainstem and tributary empirical tGMR estimates.

560 **Discussion**

561 We used tGMR to estimate escapement of Chilkat River Chinook salmon during the 2020
562 season and developed a simulation framework to evaluate potential biases arising from adult
563 sampling. Our findings suggest tGMR can produce estimates concordant with traditional mark-
564 recapture while providing increased precision, particularly when using adults representatively
565 sampled in mainstem habitat. Prior tGMR applications have similarly observed increased

566 precision with tGMR estimates in comparison to traditional methods (Rawding et al., 2014;
567 Whitmore 2016; Small et al., 2020), which arises in part from the high recapture rates afforded
568 by genetically sampling adults via their offspring. A carefully designed, representative adult
569 sampling program is crucial for avoiding violations of key tGMR assumptions (e.g., (1)
570 assuming an equal probability of adult capture and (2) assuming a closed population), and we
571 provide empirical and simulated evidence of bias that can be driven by (1) age-specific co-
572 occurring differences in both reproductive success and sampling selectivity and (2) adult dropout
573 between sample sites. Motivated by previous efforts to describe potential biases associated with
574 POP-based abundance estimates (Waples & Feutry, 2022), we leveraged parameters from our
575 Chilkat River case study to develop an individual-based model to simulate the expected direction
576 and magnitude of bias that may be encountered in tGMR applications. Through evaluation of our
577 findings, we address key uncertainties in the tGMR framework and highlight circumstances that
578 may benefit from adopting tGMR for salmon abundance estimation.

579 **Estimate Evaluation**

580 We compared six tGMR estimates - three hypergeometric and three binomial estimates -
581 to our reference abundance estimate, the traditional mark-recapture project. The hypergeometric
582 estimate using mainstem adults was most concordant with the traditional mark-recapture
583 estimate, yet the tGMR estimate had greater precision. It should be noted that the traditional
584 mark-recapture project estimates escapement of Chinook salmon ages ≥ 4 in the Chilkat River,
585 while the tGMR application estimates escapement of all age-classes, including jacks (age-3
586 males). Jacks were estimated to comprise 18% of the mainstem escapement, suggesting that if
587 the traditional mark-recapture project accounted for jacks, our reference estimate would shift
588 upwards by 18%. Subsequently, the mainstem tGMR estimate would then be underestimating

589 escapement, which may be partially explained by our simulation findings that suggest tGMR will
590 be biased between -10–13% when both reproductive success and adult sampling selectivity
591 increase with age. We observed increased reproductive success with age in the Chilkat River,
592 and despite the use of multiple gear types, it is possible that the sampling effort was still biased
593 regarding age, size, and reproductive success.

594 The binomial tGMR estimate using adults collected in the mainstem showed less
595 agreement with the traditional estimate than the hypergeometric counterpart. This departure can
596 likely be attributed to the binomial estimator being less robust to assumption violations and more
597 prone to biases as a result of following sampling with replacement (Rawding et al., 2014; Small
598 et al., 2020). Considering these observed differences within our case study and results from past
599 tGMR projects, we caution tGMR users from relying on the binomial estimator. Instead, it is
600 preferable to identify an informative panel of genomic markers for the target population to
601 confidently infer unsampled parents during parentage analysis, so that the hypergeometric
602 framework may be reliably utilized. The marker panel used here may have led to imperfectly
603 inferred unsampled parents, as evidenced by differences in captures, ‘C’, across our three
604 hypergeometric estimates (705–745 inferred unsampled parents; Table 3). This variation may be
605 driven by the marker panel’s incomplete ability to differentiate among pairs of unrelated
606 individuals, half siblings, and full siblings (Figure S4; Figure S5). While simulation results
607 indicated high statistical power of our selected markers to accurately differentiate between pairs
608 of unrelated individuals and full siblings, less power to distinguish between full- and half-
609 siblings may have limited COLONY’s ability to accurately reconstruct full- and half-sibling
610 family groups (Whitmore 2016). The hypergeometric tGMR framework can be strengthened by
611 using marker panels with sufficient power to confidently identify half-sibling relationships.

612 The tGMR estimates produced using (1) all adults sampled across the watershed and (2)
613 adults only sampled in tributaries resulted in estimates that were less concordant to the traditional
614 mark-recapture estimate. These differences emphasize that location, timing, and
615 representativeness of adult sampling is critical when conducting tGMR studies (Peterson et al.
616 2023). It is known that tributary adult samples were not representative of all Chilkat River
617 spawners, given that the distribution of samples across spawning tributaries varied greatly
618 compared to previous radiotelemetry studies (Ericksen & Chapell 2006) and the higher sampling
619 selectivity of larger, older fish. Sampling only a subset of tributary spawning locations violates
620 key assumptions, casting doubt on the veracity of the tributary tGMR estimate.

621 **Unequal Probability of Adult Capture: Violating Assumption 1**

622 Covariation in reproductive success and adult sampling selectivity has the potential to
623 violate the core tGMR assumption that all adults have the same probability of being sampled.
624 Results from our simulations indicate that bias from violating this assumption is most severe and
625 variable when both the probability of reproductive success and sampling selectivity differ with
626 age in opposing directions. For example, when reproductive success increases with age and
627 sampling selectivity is biased towards younger individuals (such as when using a fishwheel),
628 then bias can be substantial and positive. However, when both reproductive success and
629 sampling selectivity increase with age simultaneously, simulated bias is only slightly negative.
630 Variation in bias is reduced considerably under these circumstances, as the expected number of
631 POPs encountered when reproductive success and sampling selectivity simultaneously increase
632 with age becomes quite consistent. When these traits vary in opposing directions, the expected
633 number of encountered POPs ranges drastically due to random chance, which has been
634 demonstrated as the primary mechanism driving bias variability in POP-based estimators

635 (Waples & Feutry, 2022). The largely predictable and minimal nature of the bias we observed
636 when these traits covary increasingly with age makes these circumstances amenable to
637 calculating a tGMR correction factor. Additionally, it is these very conditions (increasing
638 reproductive success and sampling selectivity with age) that are most likely to be encountered
639 when enumerating salmonids. The expectation that older Pacific salmon are more reproductively
640 successful than their younger counterparts is well-documented (Koch & Narum, 2021) and
641 further supported by our results. Additionally, the most frequently used gear types are biased
642 towards selecting older, more reproductively successful individuals (Elliott & Peterson, 2018).
643 The slight negative bias driven by these co-occurring conditions will likely not perturb the
644 reliability of tGMR if identified and accounted for, at least within the limited parameter settings
645 presented in this simulation study.

646 **Dropout: Violating Assumption 2**

647 An alternative explanation for the differences between the mainstem and tributary tGMR
648 abundance estimates is adult dropout. A study that applied CKMR to a population of iteroparous
649 Atlantic salmon in Norway similarly found that variation in spatial and temporal adult sampling
650 resulted in contrasting estimates of escapement (Wacker et al., 2021). Samples collected near the
651 point of freshwater entry were thought to result in CKMR estimates of total Atlantic salmon
652 escapement, while individuals sampled during spawning surveys were described as producing an
653 estimate of only adults that had successfully migrated to upriver breeding habitat. The observed
654 parallel differences among these CKMR and tGMR findings highlight that dropout throughout
655 the adult freshwater migration can drive differences in kinship-based population estimators.

656 Dropout occurring during freshwater migrations will likely increase as climate change
657 and habitat degradation further reduce optimal conditions for the migration of spawning

658 salmonids (von Biela et al., 2022). While our simulations suggest that a 30% dropout rate is a
659 potential explanation for the discrepancy between empirical mainstem and tributary tGMR
660 estimates, it is important to note that the 95% range of abundances predicted across simulations
661 testing 15–40% rates of dropout also overlap with the empirical tributary tGMR estimate. A
662 previous radiotelemetry experiment conducted on Chilkat River Chinook salmon in 2005 found a
663 12% dropout rate (Ericksen & Chapell 2006), which is considerably lower than our point
664 estimate for 2020. Previously, the highest recorded dropout rate for Chinook salmon in Southeast
665 Alaska was 23% on the Taku River in 2016 (Richards et al., 2017). Further combining
666 radiotelemetry and tGMR studies may provide a reliable path forward to evaluate change in
667 dropout over time.

668 **Model Assumptions and Limitations**

669 Our study provides an individual-based model as a tool to quantify and correct for
670 violations of key tGMR assumptions. However, it should be emphasized that our simulation
671 framework simplifies wild Pacific salmon population dynamics and makes several notable
672 assumptions that may affect the interpretation of findings. First, sex was not considered in our
673 simulation framework; therefore, the model assumes that the focal population has an equal sex
674 ratio and no variation in age-specific reproductive success or sampling selectivity between sexes.
675 These sex-based assumptions may result in model outputs that incorrectly estimate tGMR bias
676 and variability. Therefore, future applications of this model should consider whether violations
677 of these assumptions may influence results in study systems with evidence of non-equal sex
678 ratios and sexual variation in age-specific reproductive success and sampling selectivity. We
679 chose not to include sex in our model because non-lethal sex identification of Chilkat River
680 Chinook salmon is error prone, and we were uncertain of the validity of the sex metadata

681 associated with our non-lethal adult samples. Testing the effect of sex ratios and variation in sex-
682 specific parameters would be a useful extension of our framework and could be tested in a
683 system with reliable sex data to improve the accuracy of future tGMR applications. To increase
684 the feasibility of tGMR, we encourage the continued development of marker panels that include
685 sex-associated loci for accurate and non-lethal sex identification among semelparous Pacific
686 salmon (e.g., McKinney et al. 2022).

687 Our model yields an estimate that is most akin to a single-sex binomial tGMR estimate,
688 which may limit our ability to compare simulated estimates to empirical hypergeometric
689 estimates. Incorporating the hypergeometric estimator in our simulations would have required
690 explicitly simulating genotypes for each individual, which was beyond the scope of this
691 modeling exercise. Furthermore, the single-sex binomial estimator is likely reducing the
692 simulated variation in family size compared to populations with discrete sexes. The binomial
693 estimator is dependent on the total number of POPs, which may be underestimated when
694 variation in family size is reduced. Therefore, the single-sex binomial model may overestimate
695 abundance compared to a wild population with discrete sexes and greater variation in family
696 size. As a result, estimates of dropout calculated in this study may be inflated if fewer POPs are
697 simulated than expected. Future models allowing one to compare binomial and hypergeometric
698 estimators will be useful for resolving these uncertainties.

699 **Conclusions**

700 Our empirical case study of Chilkat River Chinook salmon provides support for the use
701 of tGMR as an enumeration tool offering increased precision, accordance with traditional
702 methods, and reduced handling of adult spawners. Choosing between tGMR and traditional
703 mark-recapture methods requires weighing the benefits and costs of each method. Although

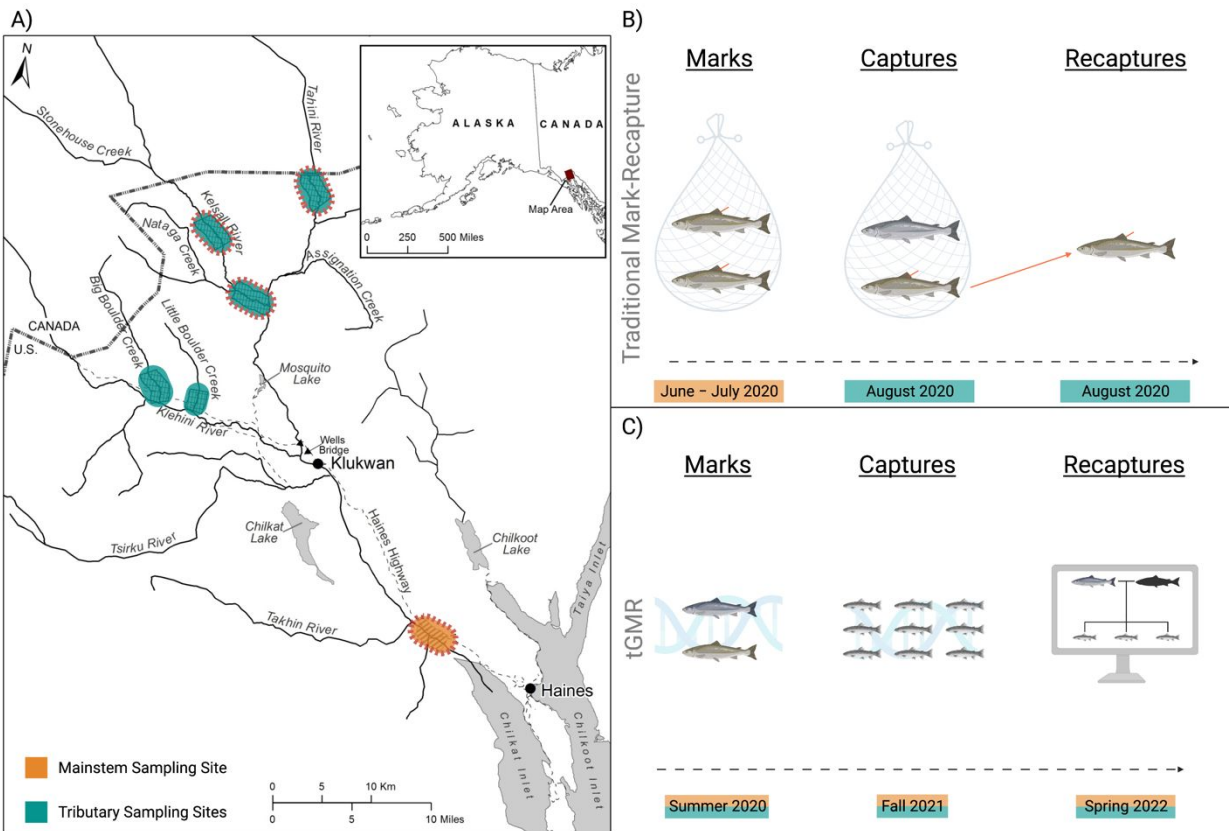
704 hardly negligible, the costs of marker development and genotyping continue to decline (Meek
705 and Larson, 2019), and not having to conduct a second adult sampling event is a significant
706 benefit when handling stress is a major concern or when the study system requires expensive and
707 challenging travel to remote locations. A major drawback of tGMR, however, is the delay
708 between adult sampling and the availability of estimates (over a year in Pacific salmon
709 applications to date, including ours). This delay precludes its use for in-season management and
710 may delay postseason run reconstruction and abundance forecasts for the next season.
711 Ultimately, the trade-offs between the two methods are likely to be case-specific, depending on
712 sampling logistics and the information needs for management. Because tGMR has emerged
713 recently, studies that compare both tGMR and traditional methods such as ours and others
714 (Rawding et al., 2014; Whitmore 2016; Small et al., 2020) are particularly useful for evaluating
715 these trade-offs.

716 Our case study and simulation analysis aimed to illuminate uncertainties surrounding
717 violations of (1) the equal probability of capture assumption and (2) the closed population
718 assumption. We assert that these two assumptions are those most likely to be violated when
719 enumerating Pacific salmon; however, further work evaluating the remaining mark-recapture
720 assumptions will continue to inform the utility of tGMR. Specifically, we recommend future
721 efforts investigate the relative importance of random versus non-random offspring sampling in a
722 tGMR framework, as this may be useful for determining optimal sampling strategies required to
723 achieve unbiased escapement estimates.

724 The individual-based model detailed here offers a simple and flexible framework for
725 simulating the accuracy and precision of tGMR estimation across an array of demographic and
726 sampling scenarios. Enumeration of spawning populations using tGMR can provide widely

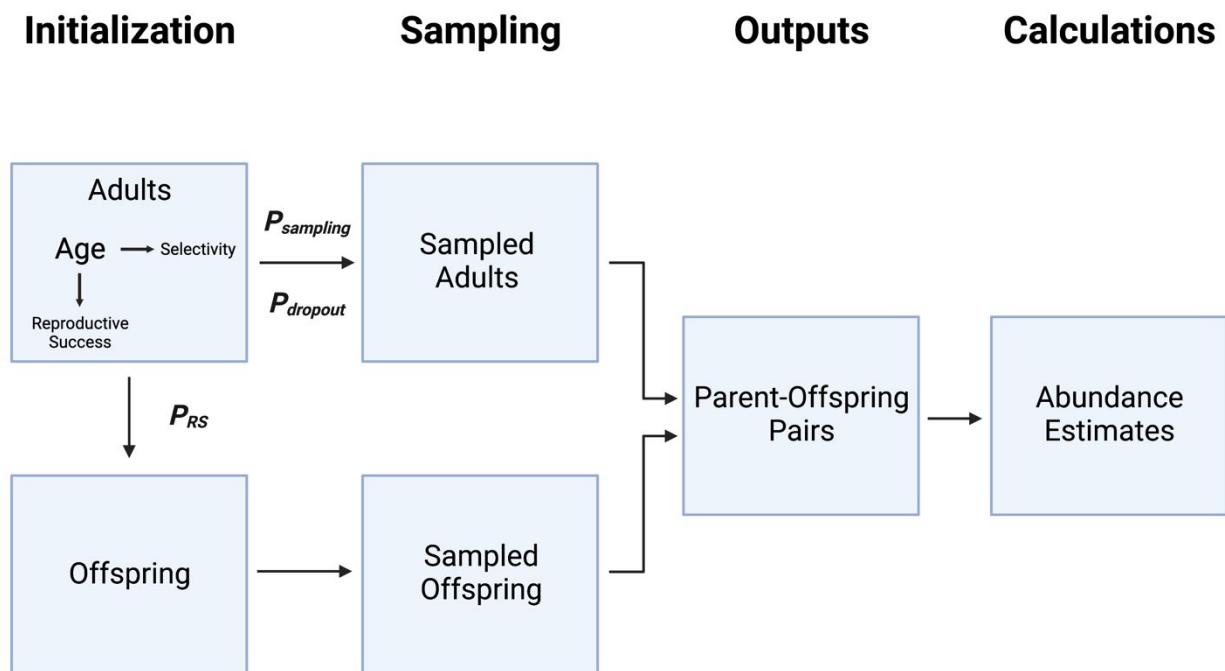
727 applicable benefits to agencies seeking to increase the effectiveness of escapement-based
 728 management programs, while reducing invasive sampling. Future efforts to enumerate salmonids
 729 expressing complex life histories and various population sizes, should additionally be explored to
 730 determine tGMR's reliability for enumerating a diversity of semelparous populations.

731 Figures



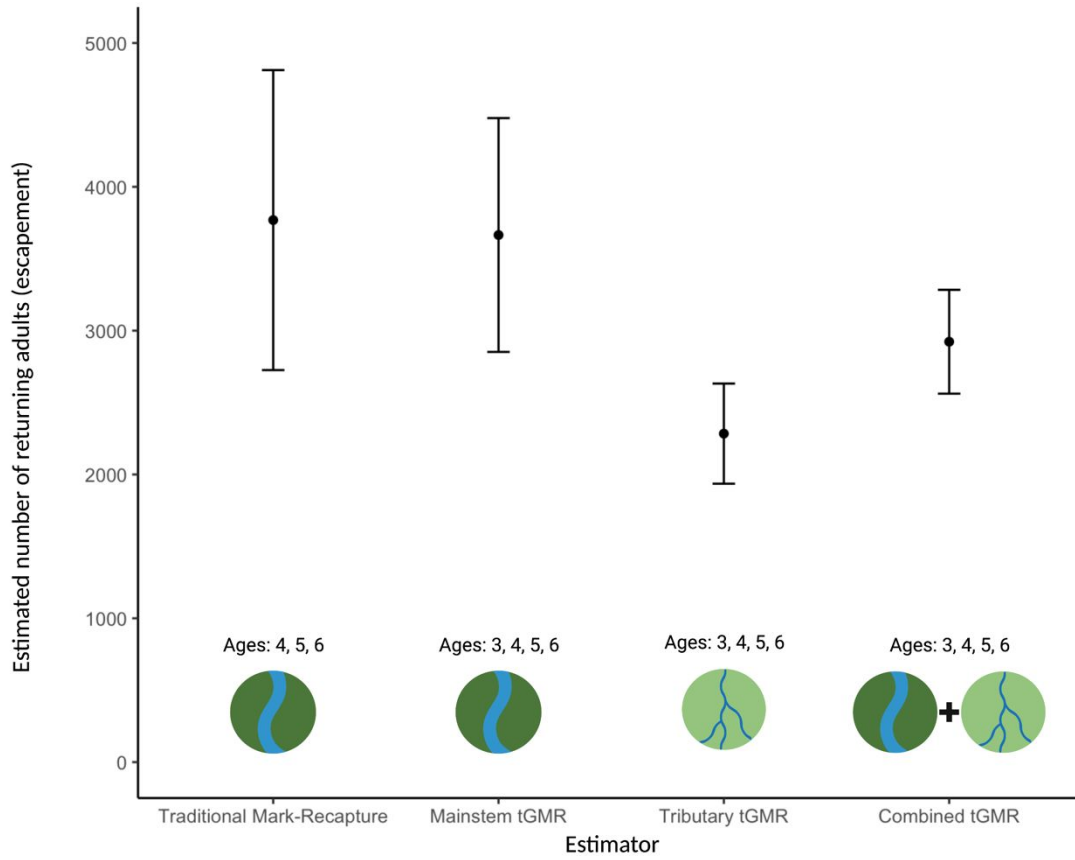
732

733 Figure 1: A) Map of the Chilkat River watershed near Haines, AK. Chinook salmon were
 734 sampled in the mainstem (orange) and tributaries (blue). Sampling areas with a dashed red
 735 border denote locations where both adult and juvenile Chinook salmon were collected. Areas
 736 without the dashed red border indicate that only adults were sampled. B) Diagram of a traditional
 737 mark-recapture program used to estimate the escapement of Chilkat River Chinook salmon in
 738 2020. C) Diagram of the trans-generational genetic mark-recapture (tGMR) framework used to
 739 estimate escapement of Chilkat River Chinook salmon in 2020, created with BioRender.com.



740

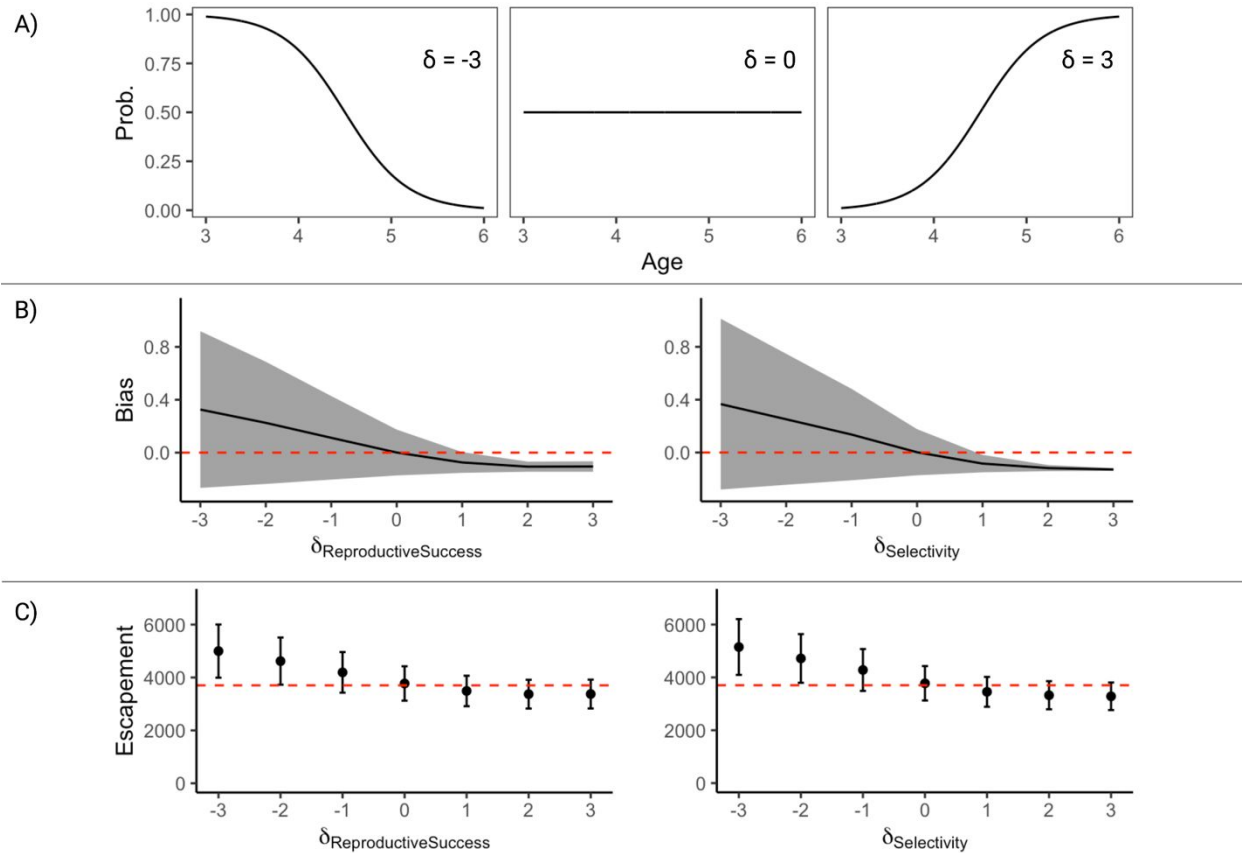
741 Figure 2: Schematic of our individual-based model workflow to quantify the reliability of trans-
 742 generational genetic mark-recapture (tGMR) for Chilkat River Chinook salmon under varying
 743 demographic and sampling scenarios. Created with BioRender.com.



744

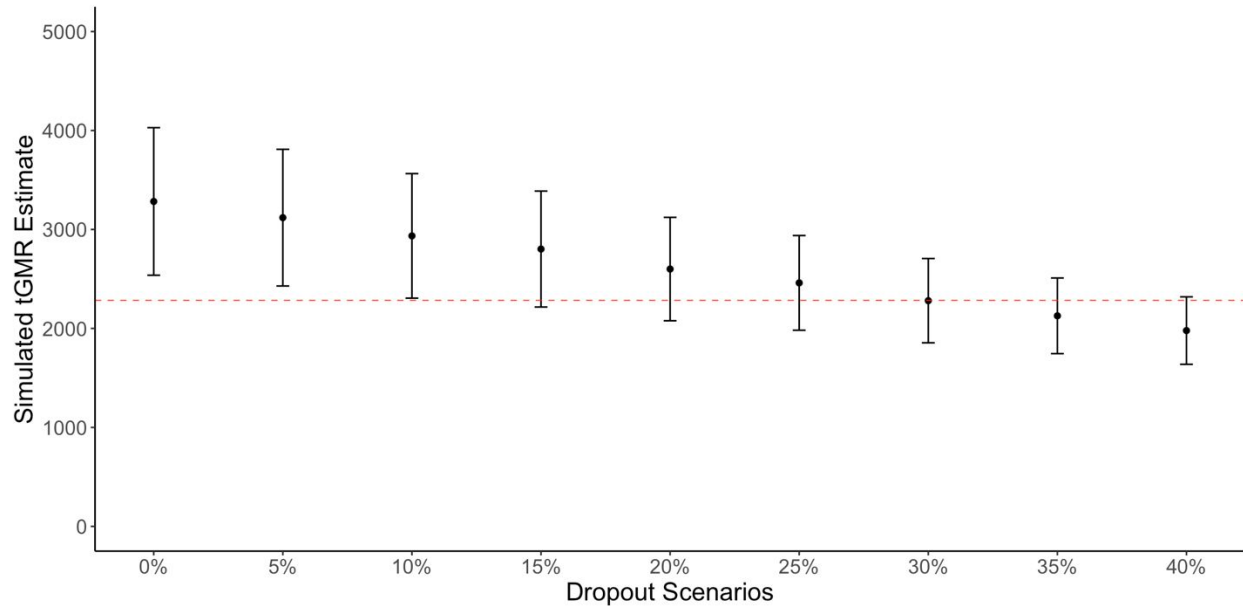
745 Figure 3: Estimated number of returning adults (escapement; y-axis) from four different
 746 estimation methods (x-axis) of adult Chilkat River Chinook salmon. Estimation methods include
 747 a traditional mark-recapture survey (left), which we compare to three hypergeometric tGMR
 748 estimates (right), quantified using samples collected on the river mainstem, tributaries, or both.
 749 Estimates are bounded by 95% confidence intervals. Icons created with BioRender.com.

750



751

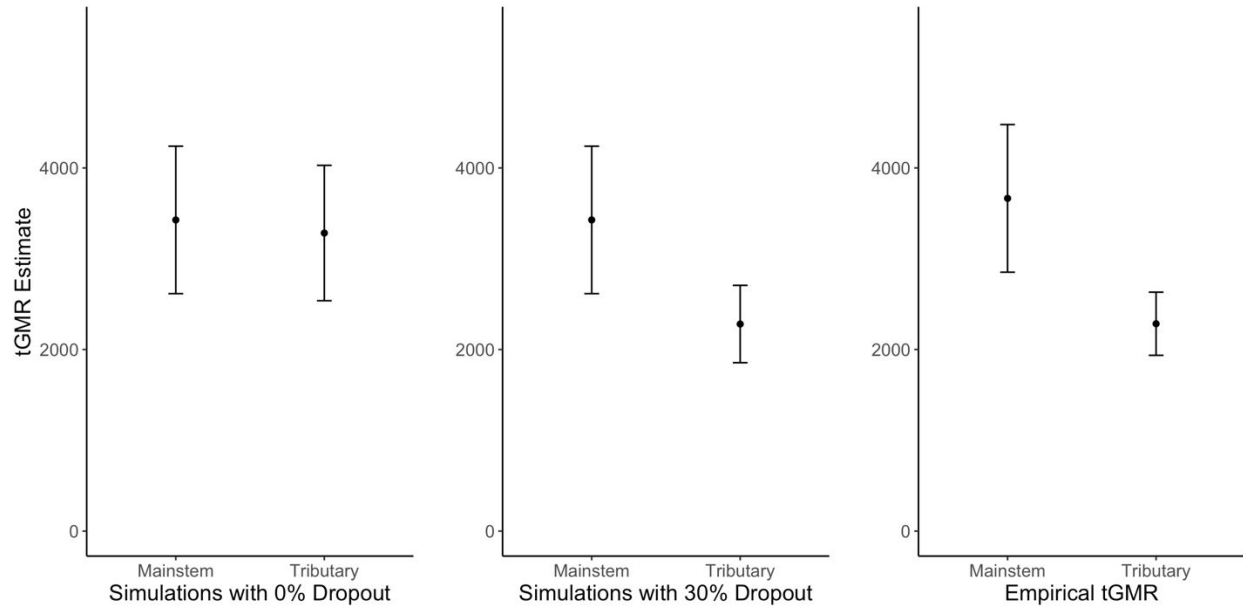
752 Figure 4: A) Example scenarios varying the slope variable (δ) to quantify reproductive success
 753 and selectivity probabilities (y-axis) for different ages (x-axis) of Chilkat River Chinook salmon
 754 (Equation 7 in the text). B) Expected bias (y-axis) in trans-generational genetic mark-recapture
 755 (tGMR) estimates resulting from age-specific differences (x-axis) in reproductive success (left)
 756 and sampling selectivity (right). Shaded area indicates the range of bias predicted by 95% of
 757 simulations. Red dashed line represents zero bias. C) Simulated average tGMR estimates, using a
 758 single-sex binomial framework, and the 95% range of abundances predicted across 1,000
 759 iterations for each δ scenario. The red dashed line represents the true simulated population size.



760

761 Figure 5: Simulated escapement (y-axis) for Chilkat River Chinook salmon using a single-sex
762 binomial trans-generational genetic mark-recapture (tGMR) estimate parameterized with varying
763 rates of dropout (x-axis) between the mainstem and tributary sampling areas from 0% to 40%.
764 Error bars indicate the 95% range of abundances predicted across 1,000 iterations for each
765 dropout scenario. We compare these dropout scenarios to our empirical escapement estimate (red
766 dashed line), quantified using a hypergeometric tGMR approach on adults sampled in the upriver
767 spawning tributaries.

768



769

770 Figure 6: Simulated escapement (y-axes) of Chilkat River Chinook salmon comparing 0%
 771 dropout (left) and 30% dropout scenarios (middle) to empirical hypergeometric mainstem and
 772 tributary estimates (right), while accounting for differences in age composition and selectivity.
 773 Error bars for simulations indicate the 95% range of abundances predicted across 1,000 iterations
 774 for each scenario; error bars for empirical estimates indicate 95% confidence intervals.

775 Tables

776 Table 1: Input parameters and example values for individual-based simulations of Chilkat River
 777 Chinook salmon.

<u>Argument</u>	<u>Definition</u>	<u>Example Values</u>
N_{adults}	Adult census size	3,702
$N_{\text{offspring}}$	Juvenile census size	480,000
n_{adults}	Adult sample size	581
$n_{\text{offspring}}$	Offspring sample size	682
Ages	Adult ages	3, 4, 5, 6
P_{age}	Adult age structure probability	0.1, 0.14, 0.64, 0.12
P_{RS}	Age-specific reproductive success probability	0.07, 0.17, 0.28, 0.38
P_{sampling}	Age-specific sampling probability	0.03, 0.30, 0.38, 0.29
P_{dropout}	Age-specific probability of removal of individuals from the population between mainstem and tributary sampling events	0.05

Proportion _{dropout}	Proportion of adults that are randomly removed from the population between simulated mainstem and tributary sampling events	0.30
Iterations	Number of iterations performed for each unique combination of input parameters	1,000
Scenario	Scenario identifier	1
δ_{RS}	Slope of a logistic function predicting age-specific probabilities of having offspring	-3, -2, -1, 0, 1, 2, 3
δ_{sampling}	Slope of a logistic function predicting age-specific probabilities of being sampled	-3, -2, -1, 0, 1, 2, 3

778

779 Table 2: Age structure and selectivity for adult Chinook salmon, separated by adult age-class,
780 across lower mainstem and upriver tributary sampling efforts.

Parameter	Age 3	Age 4	Age 5	Age 6
Mainstem Age Structure	18%	12%	60%	10%
Mainstem Selectivity	18%	12%	60%	10%
Tributary Age Structure	1%	16%	69%	14%
Tributary Selectivity	1%	34%	29%	36%

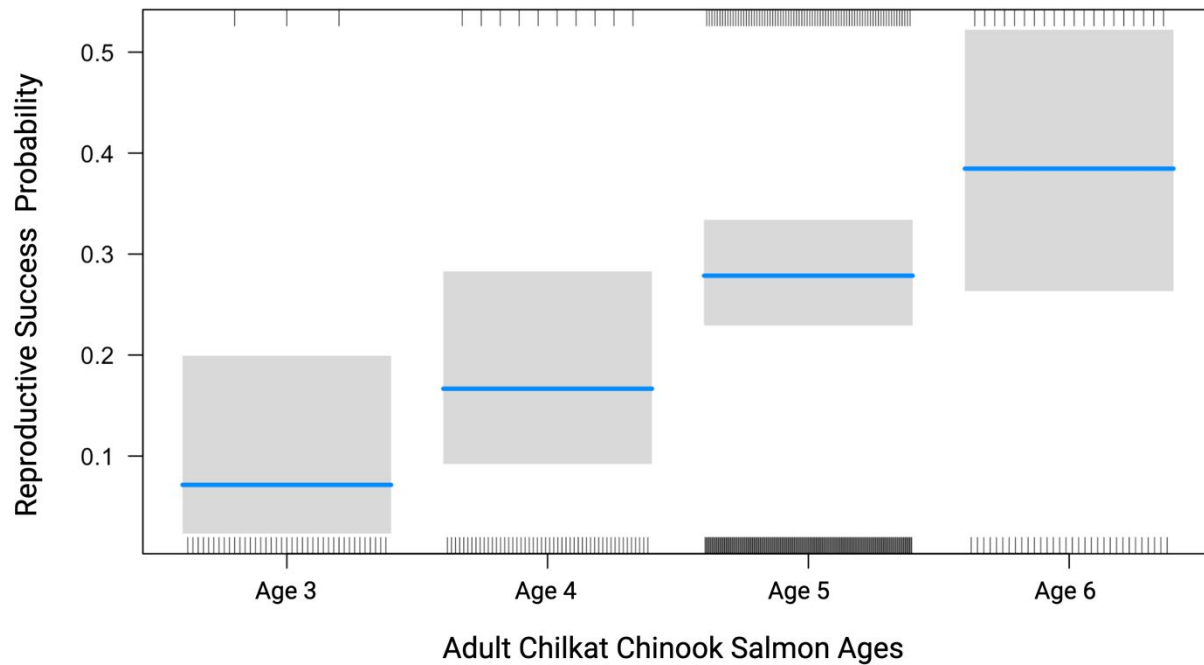
781

782 Table 3: Comparison of traditional and trans-generational genetic mark-recapture (tGMR)
783 estimators for Chilkat River Chinook salmon. The traditional mark-recapture estimate is
784 provisional, based on mark (M), capture (C), and recapture (R) values not currently being
785 published (Elliott & Peterson, 2022).

Estimator	M	C	R	Estimate	95% CI	CV
Traditional Mark-Recapture (Adults \geq age 4)	n/a	n/a	n/a	3,769	(2,726 – 4,812)	14%
Hypergeometric tGMR (All adults)	583	745	148	2,923	(2,562 – 3,284)	6%
Hypergeometric tGMR (Mainstem adults)	295	705	56	3,665	(2,852 – 4,478)	11%
Hypergeometric tGMR (Tributary adults)	306	721	96	2,284	(1,936 – 2,632)	8%
Binomial tGMR (All adults)	583	1,364	237	3,344	(2,958 – 3,729)	6%
Binomial tGMR (Mainstem adults)	295	1,364	83	4,794	(3,806 – 5,781)	11%

Binomial tGMR (Tributary adults)	306	1,364	165	2,516	(2,159 – 2,874)	7%
----------------------------------	-----	-------	-----	-------	-----------------	----

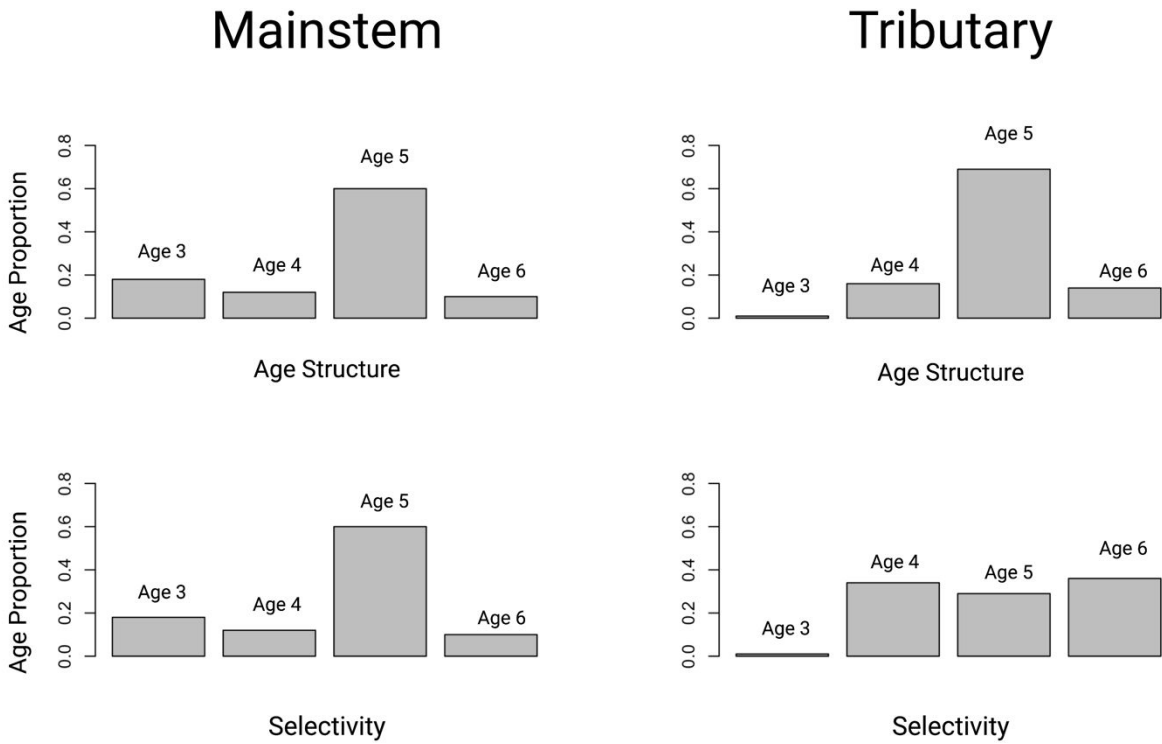
786

787 **Supplementary Figures**

788

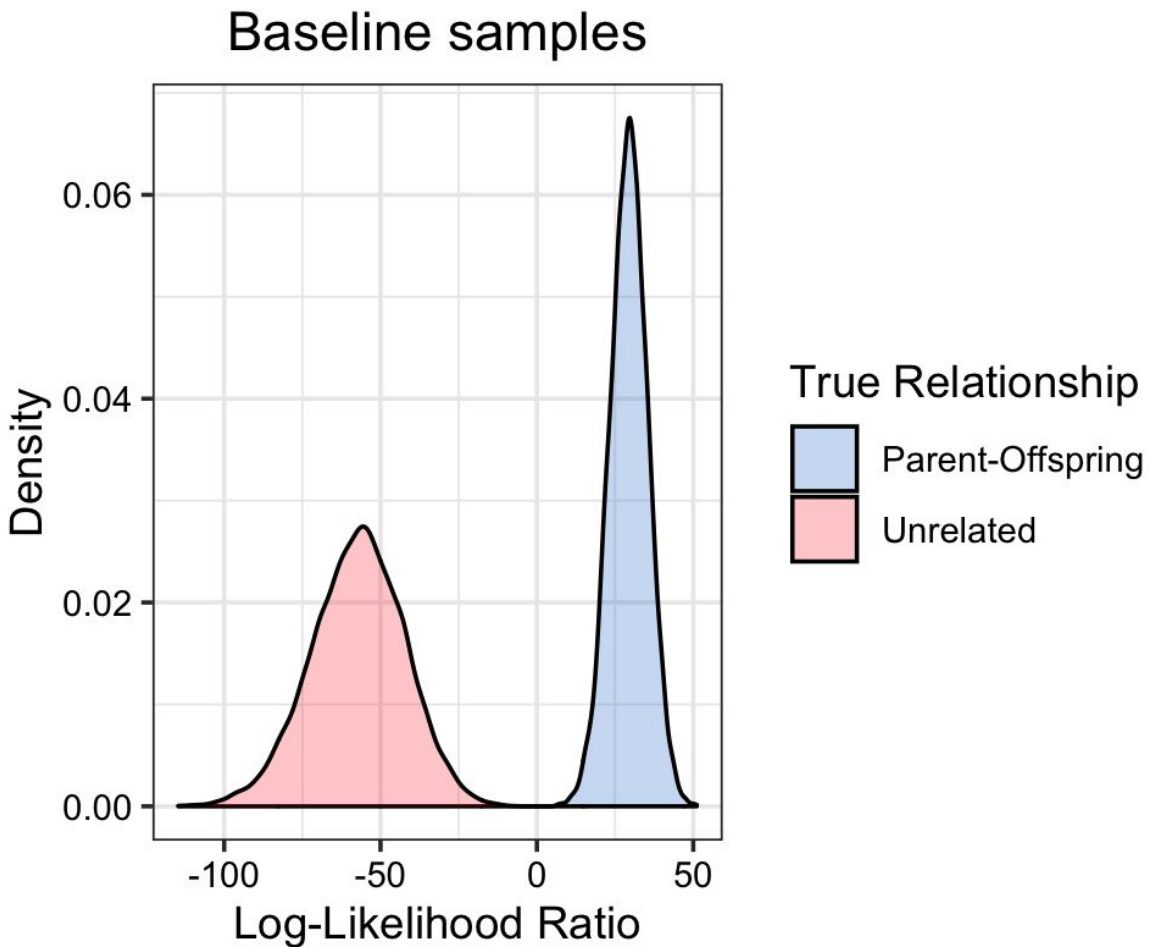
789 Figure S1: The proportion of individuals that had at least one offspring (y-axis) at a given age (x-
 790 axis). Blue horizontal lines indicate the mean P_{RS} values and the grey shaded area represents the
 791 confidence band associated with the mean value.

792



793

794 Figure S2: TOP) Proportion of total population size (y-axes) for each age class (x-axes) specific
 795 to each sampling habitat (mainstem, left; tributary, right). BOTTOM) Proportion of population
 796 sampled (y-axes) for each age class (x-axes) for each sampling habitat (mainstem, left; tributary,
 797 right).



798

799 Figure S3: Distributions of log-likelihood ratios, generated using CKMRsim, between parent-
800 offspring pairs (blue) and unrelated pairs (red) of Chinook salmon. Baseline samples were
801 genotyped at 301 SNPs and 13 microsatellite loci, however only 255 SNPs were retained for
802 analyses. Using the available baseline samples from 2004, this CKMRsim analysis simulated the
803 power of 255 SNPs plus a single multiplex of 5 microsatellite loci for valid parentage inference.

804

805

806

807

808

809

810

811

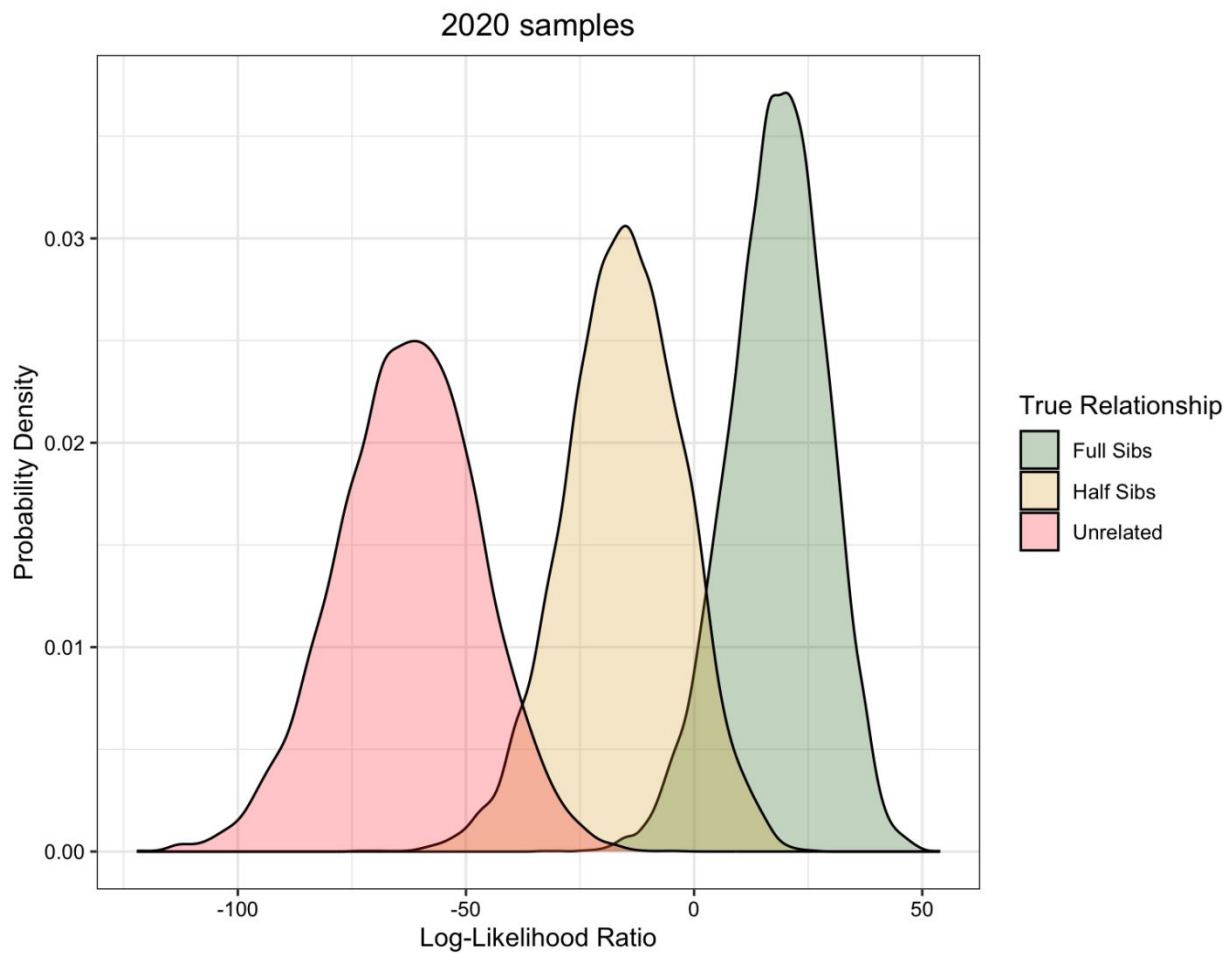
812

813

814

815

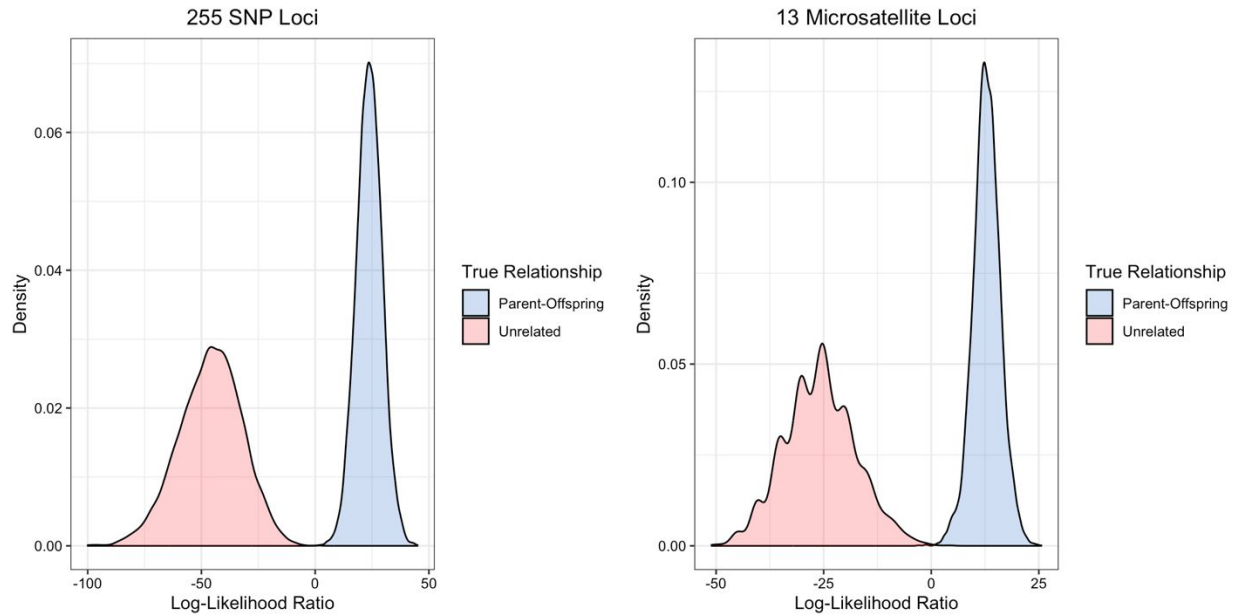
816



817

818 Figure S4: The log-likelihood ratio distribution, generated using CKMRsim, among unrelated
819 pairs (red), half-sibling pairs (yellow), and full-sibling pairs (green) of Chinook salmon. Samples
820 from 2020 were genotyped at 299 SNPs and 5 microsatellite loci. This CKMRsim analysis
821 simulated the power of 254 SNPs plus a single multiplex of 5 microsatellite loci for valid sibship
822 inference.

823



824
 825 Figure S5: Distributions of log-likelihood ratios, generated using CKMRsim, between parent-
 826 offspring pairs (blue) and unrelated pairs (red) of Chinook salmon. The left panel displays log-
 827 likelihood distributions for these relationships using 255 SNPs, while the right panel shows the
 828 same information using 13 microsatellites.

829
 830
 831
 832
 833
 834
 835
 836
 837
 838
 839
 840

841 **Supplementary Tables**

842 Table S1: Input parameters for three implementations of the parentage analysis software,
 843 COLONY. The number of Chilkat River Chinook salmon adults when using mainstem samples
 844 (implementation 2, not shown) was 295, and the Prob of dam and sire in candidates was 0.09.
 845 The number of adults when using tributary samples (implementation 3, not shown) was 306, and
 846 the Prob of dam and sire in candidates was 0.10.

Parameter	Implementation 1: All Adults and All Juveniles
Number of adults in the sample	583

847	Number of offspring in the sample	682
848	Number of loci	259
849	Seed for random number generator	1234
850	Not updating/updating allele frequency	Updating
851	Dioecious/monoecious species	Dioecious
852	Inbreeding absent/present	Absent
853	Diploid species/haplodiploid species	Diploid
854	Polygamy/monogamy for males & females	Polygamy
855	Clone inference	No
856	Scale full sibship	Yes
857	Sibship prior	Weak
858	Unknown/known population allele frequency	Unknown
859	Number of runs	1
860	Length of run	Medium
861	Monitor method	Time in seconds
862	Monitor interval	Seconds
863	Version	Windows
864	Likelihood method	Full-Likelihood
865	Precision	Medium
866	Prob of Dad (and Mum) in candidates	0.23

864

865

866

867

868

869 Table S2: Sample sizes of genotyped Chilkat River Chinook salmon in each sampling event and
 870 the number of individuals removed due to missing data, duplicate samples, and excessive
 871 heterozygosity. Note that duplicates found in “all adults” are due to recaptures between the
 872 mainstem and tributary sampling events.

Sample Collection	Genotyped	Missing Data	Duplicates	Excessive heterozygosity	Final Dataset
All adults	641	0	19	39	583

Mainstem Adults	312	0	0	17	295
Tributary Adults	329	0	1	22	306
Juveniles	700	10	1	7	682

873

874 Table S3 Samples sizes and locations for adult Chilkat River Chinook samples collected in 2020
875 with genotypes passing quality assurance steps.

Sample Location	Number of Adults in Final Dataset
Mainstem Fishwheel (Chilkat River)	150
Mainstem Gillnet (Chilkat River)	145
Kelsall (Chilkat Tributary)	79
Tahini (Chilkat Tributary)	210
Klehini (Chilkat Tributary)	17

876

877 Table S4 Samples sizes and locations for juvenile Chilkat River Chinook samples collected in
878 2021 with genotypes passing quality assurance steps.

Sample Location	Number of Juveniles in Final Dataset
Mainstem (Chilkat River)	191
Kelsall (Chilkat Tributary)	247
Tahini (Chilkat Tributary)	244

879

880 Table S5: Key paramters and results for the dropout simulations for Chilkat River Chinook
881 salmon.

Scenario	P_{sampling}	Adults	Dropout %	Estimate	95% Range of Abundances
1 (Mainstem)	0.18, 0.12, 0.60, 0.10	295	0	3,427	2,615 – 4,239
2 (Tributary)	0.01, 0.34, 0.29, 0.36	306	0	3,283	2,538 – 4,028
3 (Tributary)	0.01, 0.34, 0.29, 0.36	306	5	3,119	2,429 – 3,810
4 (Tributary)	0.01, 0.34, 0.29, 0.36	306	10	2,935	2,306 – 3,564

5 (Tributary)	0.01, 0.34, 0.29, 0.36	306	15	2,802	2,216 – 3,388
6 (Tributary)	0.01, 0.34, 0.29, 0.36	306	20	2,600	2,078 – 3,123
7 (Tributary)	0.01, 0.34, 0.29, 0.36	306	25	2,460	1,982 – 2,938
8 (Tributary)	0.01, 0.34, 0.29, 0.36	306	30	2,281	1,855 – 2,706
9 (Tributary)	0.01, 0.34, 0.29, 0.36	306	35	2,128	1,745 – 2,510
10 (Tributary)	0.01, 0.34, 0.29, 0.36	306	40	1,978	1,638 – 2,319

882

883 **Supplementary Material**884 **Parentage Power Analysis Methods**

885 We used previously collected baseline genotype data from adult Chilkat River Chinook
886 salmon sampled in 2004 (K. Shedd & Gilk-Baumer, 2021) and the R package *CKMRsim* (Dr.
887 Eric Anderson <https://github.com/eriqande/CKMRsim>) to evaluate the power of various
888 combinations of genetic markers to sufficiently detect all parent-offspring relationships (false
889 negative rate < 0.0001, for a false positive rate = 100 times the reciprocal of the number of
890 anticipated pairwise comparisons of parents and offspring). These available baseline samples
891 were genotyped for 301 single nucleotide polymorphism (SNP) genetic markers using
892 Genotyping-in-Thousands by sequencing (GT-seq; Campbell et al., 2015) in combination with
893 13 microsatellite loci from the Genetic Analysis of Pacific Salmon (GAPS) panel (Seeb et al.,
894 2007; Moran et al., 2013). The 301 SNP GT-seq panel was based off of the 299 SNP v3.0 GT-
895 seq panel developed by the Columbia River Inter-tribal Fish Commission Hagerman Genetics
896 Laboratory (Hess et al., 2014) with two additional SNPs (*Ots_uwsnp640165* and
897 *Ots_uwsnp670329*) that are associated with the run timing gene GREB1L (Prince et al., 2017).
898 We used *CKMRsim* to calculate population allele frequencies from baseline samples, simulate

899 multi-locus genotypes for different relationships, and evaluate the statistical power of a given
900 marker set (254 SNPs and 5 microsatellite loci) for identifying valid parentage assignments
901 (Figure S3).

902 **Parentage Power Analysis Results**

903 When simulating the false positive and false negative rates of parentage assignments
904 associated with various combinations of GAPS microsatellite multiplexes in conjunction with a
905 GT-seq SNP panel in *CKMRsim*, we determined that a single multiplex of five microsatellite loci
906 accompanied by the SNP panel would provide ample power for valid parentage assignments.
907 Figure 4 shows that the distribution of log-likelihood ratios for POPs versus unrelated pairs have
908 minimal overlap, indicating adequate statistical power for differentiating between these two
909 groups. Our evaluation of parentage panels in *CKMRsim* was based on the criteria of requiring a
910 false positive rate that is 10 times lower than the reciprocal of the number of comparisons we
911 made $(0.1 \times (641 \text{ adults} \times 700 \text{ parr}))^{-1} = 2.2^{-5}$ (recommendation from Eric Anderson, author of
912 *CKMRsim*). Using ADF&G's baseline samples of Chilkat River Chinook salmon, we observed a
913 simulated false positive rate of 2.34^{-7} and a false negative rate of 0.0006 in *CKMRsim* associated
914 with our proposed panel.

915 Once the 2020 adult samples were genotyped, we re-ran the *CKMRsim* analysis to
916 evaluate how similar the final panels performed for parentage analysis between the baseline and
917 2020 samples. As expected, the contemporary *CKMRsim* results indicated that the 2020 samples
918 provided concordant statistical power for parentage inference, simulating a false positive rate of
919 $3.98e^{-7}$ and a false negative rate of 0.0001.

920 **Data Archiving/Accessibility Statement:** Data for this study are available at:

921 https://github.com/swrosenbaum/tGMR_simulations

922 **Literature Cited**

923 Adkison, M. D. (2022). A Review of Salmon Spawner-Recruitment Analysis: The Central Role

924 of the Data and Its Impact on Management Strategy. *Reviews in Fisheries Science &*

925 *Aquaculture*, 30(3), 391–427. <https://doi.org/10.1080/23308249.2021.1972086>

926 Anderson, J. H., Faulds, P. L., Atlas, W. I., & Quinn, T. P. (2013). Reproductive Success of

927 Captively Bred and Naturally Spawned Chinook Salmon Colonizing Newly Accessible

928 Habitat. *Evolutionary Applications*, 6(2), 165–179. <https://doi.org/10.1111/j.1752->

929 4571.2012.00271.x

930 Bailey, N. T. J. (1951). On Estimating the Size of Mobile Populations from Recapture Data.

931 *Biometrika*. 293–306.

932 Beamish, R. (2022). The need to see a bigger picture to understand the ups and downs of Pacific

933 salmon abundances. *ICES Journal of Marine Science*, 79, 1005–1014.

934 <https://doi.org/10.1093/icesjms/fsac036>

935 Berdahl, A. M., Kao, A. B., Flack, A., Westley, P. A. H., Codling, E. A., Couzin, I. D., Dell, A.

936 I., & Biro, D. (2018). Collective animal navigation and migratory culture: From

937 theoretical models to empirical evidence. *Philosophical Transactions of the Royal Society*

938 *B: Biological Sciences*, 373(1746), 20170009. <https://doi.org/10.1098/rstb.2017.0009>

939 Biela, V. R., Sergeant, C. J., Carey, M. P., Liller, Z., Russell, C., Quinn-Davidson, S., Rand, P.

940 S., Westley, P. A. H., & Zimmerman, C. E. (2022). Premature Mortality Observations

941 among Alaska's Pacific Salmon During Record Heat and Drought in 2019. *Fisheries*,

942 47(4), 157–168. <https://doi.org/10.1002/fsh.10705>

- 943 Bonner, S. J., Morgan, B. J. T., & King, R. (2010). Continuous Covariates in Mark-Recapture-
944 Recovery Analysis: A Comparison of Methods. *Biometrics*, *66*(4), 1256–1265.
945 <https://doi.org/10.1111/j.1541-0420.2010.01390.x>
- 946 Bowerman, T., Keefer, M. L., & Caudill, C. C. (2016). Pacific Salmon Prespawn Mortality:
947 Patterns, Methods, and Study Design Considerations. *Fisheries*, *41*(12), 738–749.
948 <https://doi.org/10.1080/03632415.2016.1245993>
- 949 Bravington, M. V., Skaug, H. J., & Anderson, E. C. (2016). Close-Kin Mark-Recapture.
950 *Statistical Science*, *31*(2). <https://doi.org/10.1214/16-STS552>
- 951 Bromaghin, J. F. (2005). A Versatile Net Selectivity Model, With Application to Pacific Salmon
952 and Freshwater Species of the Yukon River, Alaska. *Fisheries Research*, *74*(1–3), 157–
953 168. <https://doi.org/10.1016/j.fishres.2005.03.004>
- 954 Campbell, N. R., Harmon, S. A., & Narum, S. R. (2015). Genotyping-in-Thousands by
955 Sequencing (GT-seq): A Cost Effective SNP Genotyping Method Based on Custom
956 Amplicon Sequencing. *Molecular Ecology Resources*, *15*(4), 855–867.
957 <https://doi.org/10.1111/1755-0998.12357>
- 958 Chapman, D. G. (1951). Some Properties of Hypergeometric Distribution with Application to
959 Zoological Census. *University of California Publications Statistics*, *1*, 131–160.
- 960 Chapell, R. S. 2014. Production, escapement, and juvenile tagging of Chilkat River Chinook
961 salmon in 2011. Alaska Department of Fish and Game, Fishery Data Series No. 14-55,
962 Anchorage.
- 963 Chinook Technical Committee. (2023). Annual Report of Catch and Escapement. For 2022.
964 Pacific Salmon Commission. Report TCCHINOOK, (23)-02. Vancouver, BC.

- 965 Clark, J. H., McGregor, A., Mecum, R. D., Krasnowski, P., & Carroll, A. M. (2006). *The*
966 *Commercial Salmon Fishery in Alaska*. *Alaska Fishery Research Bulletin*, 12(1), 1–46.
- 967 Elliott, B. W. (2022). *Operational plan: Chilkat River Chinook Salmon Escapement Studies in*
968 *2020*. 68. Alaska Department of Fish and Game, Division of Sport Fish, Regional
969 Operational Plan No. ROP.SF.1J.2022.06, Anchorage.
- 970 Elliott, B. W., & Peterson, R. L. (2018). *Production and Harvest of Chilkat River Chinook and*
971 *Coho Salmon, 2018–2019*. Alaska Department of Fish and Game, Regional Operational
972 Plan No. ROP.SF.1J.2018.10, Anchorage.
- 973 Elliott, B. W., & Peterson, R. L. (2022). *Production and Harvest of Chilkat River Chinook and*
974 *Coho Salmon, 2020–2021*. Alaska Department of Fish and Game, Division of Sport Fish,
975 Regional Operational Plan No. ROP.SF.1J.2022.26, Anchorage.
- 976 Ericksen, R. P., and McPherson, S. A. (2004). *Optimal Production of Chinook Salmon from the*
977 *Chilkat River*. Alaska Department of Fish and Game, Fishery Manuscript No. 04-01,
978 Anchorage.
- 979 Ericksen, R. P., and Chapwell, R. S. (2006). *Production and spawning distribution of Chilkat*
980 *River Chinook salmon in 2005*. Alaska Department of Fish and Game, Fishery Data
981 Series No. 06–76, Anchorage.
- 982 Helfield, J. M., & Naiman, R. J. (2006). Keystone Interactions: Salmon and Bear in Riparian
983 Forests of Alaska. *Ecosystems*, 9(2), 167–180. [https://doi.org/10.1007/s10021-004-0063-](https://doi.org/10.1007/s10021-004-0063-5)
984 5
- 985 Hess, J. E., Campbell, N. R., Matala, A. P., & Narum, S. R. (2014). *Genetic Assessment of*
986 *Columbia River Stocks*. Columbia River Inter-Tribal Fish Commission annual report.

- 987 Koch, I. J., & Narum, S. R. (2021). An Evaluation of the Potential Factors Affecting Lifetime
988 Reproductive Success in Salmonids. *Evolutionary Applications*, *14*(8), 1929–1957.
989 <https://doi.org/10.1111/eva.13263>
- 990 Koo, T. S. Y. (1955). Biology of the red salmon, *Oncorhynchus nerka* (Walbaum), of Bristol
991 Bay, Alaska, as revealed by a study of their scales. Ph.D. thesis, University of
992 Washington, Seattle.
- 993 Lin, J. E., Hard, J. J., Hilborn, R., & Hauser, L. (2017). Modeling local adaptation and gene flow
994 in sockeye salmon. *Ecosphere*, *8*(12). <https://doi.org/10.1002/ecs2.2039>
- 995 Lum, J. L., and Fair, L. (2018). *Chilkat River and King Salmon River King Salmon Stock Status
996 and Action Plan, 2018*. Alaska Department of Fish and Game, Regional Information
997 Report No 1J18-05, Douglas
- 998 May, S. A., Hard, J. J., Ford, M. J., Naish, K. A., & Ward, E. J. (2023). Assortative Mating for
999 Reproductive Timing Affects Population Recruitment and Resilience in a Quantitative
1000 Genetic Model. *Evolutionary Applications*, *16*(3), 657–672.
1001 <https://doi.org/10.1111/eva.13524>
- 1002 McKinney, G. J., Pascal, C. E., Templin, W. D., Gilk-Baumer, S. E., Dann, T. H., Seeb, L. W., &
1003 Seeb, J. E. (2020). Dense SNP Panels Resolve Closely Related Chinook Salmon
1004 Populations. *Canadian Journal of Fisheries and Aquatic Sciences*, *77*(3), 451–461.
1005 <https://doi.org/10.1139/cjfas-2019-0067>
- 1006 McPherson, S., Bernard, D., Clark, J. H., Pahlke, K., Jones, E., Hovanisian, J. D., Weller, J., &
1007 Ericksen, R. (2003). *Stock Status and Escapement Goals for Chinook Salmon Stocks in
1008 Southeast Alaska*. Alaska Department of Fish and Game, Special Publication No. 03-01,
1009 Anchorage.

- 1010 Meek, M. H., & Larson, W. A. (2019). The Future is Now: Amplicon Sequencing and Sequence
1011 Capture Usher in the Conservation Genomics Era. *Molecular Ecology Resources*, *19*(4),
1012 795–803. <https://doi.org/10.1111/1755-0998.12998>
- 1013 Moore, J. W. (2006). Animal Ecosystem Engineers in Streams. *BioScience*, *56*(3), 237–246.
- 1014 Moran, P., Teel, D. J., Banks, M. A., Beacham, T. D., Bellinger, M. R., Blankenship, S. M.,
1015 Candy, J. R., Garza, J. C., Hess, J. E., Narum, S. R., Seeb, L. W., Templin, W. D.,
1016 Wallace, C. G., & Smith, C. T. (2013). Divergent Life-history Races Do Not Represent
1017 Chinook Salmon Coast-Wide: The importance of Scale in Quaternary Biogeography.
1018 *Canadian Journal of Fisheries and Aquatic Sciences*, *70*(3), 415–435.
1019 <https://doi.org/10.1139/cjfas-2012-0135>
- 1020 Naiman, R. J., Bilby, R. E., Schindler, D. E., & Helfield, J. M. (2002). Pacific Salmon, Nutrients,
1021 and the Dynamics of Freshwater and Riparian Ecosystems. *Ecosystems*, *5*(4), 399–417.
1022 <https://doi.org/10.1007/s10021-001-0083-3>
- 1023 Parsons, A., & Skalski, J. (2010). Quantitative Assessment of Salmonid Escapement Techniques.
1024 *Reviews in Fisheries Sciences*, *18.4*, 301–314.
- 1025 Peterson, R., Shedd, K., Frost, N., Elliott, B., & Richards, P. (2023). *Estimating Adult Chinook*
1026 *Salmon Abundance on the Chilkat and Unuk Rivers Using Transgenerational Genetic*
1027 *Mark–Recapture*. Alaska Department of Fish and Game, Divisions of Sport Fish and
1028 Commercial Fisheries, Regional Operational Plan No. ROP.SF.1J.2023.02, Douglas.
- 1029 Piccolo, J. J., Adkison, M. D., & Rue, F. (2009). Linking Alaskan Salmon Fisheries Management
1030 with Ecosystem-based Escapement Goals: A Review and Prospectus. *Fisheries*, *34*(3),
1031 124–134. <https://doi.org/10.1577/1548-8446-34.3.124>

- 1032 Pradel, R. (1996). Utilization of Capture-Mark-Recapture for the Study of Recruitment and
1033 Population Growth Rate. *Biometrics*, 52(2), 703. <https://doi.org/10.2307/2532908>
- 1034 Prince, D. J., Saglam, I. K., Hotaling, T. J., Spidle, A. P., & Miller, M. R. (2017). The
1035 Evolutionary Basis of Premature Migration in Pacific Salmon Highlights the Utility of
1036 Genomics for Informing Conservation. *Science Advances*, 3(8), e1603198.
- 1037 R Core Team (2023). *_R: A Language and Environment for Statistical Computing_*. R
1038 Foundation for Statistical Computing, Vienna, Austria. <<https://www.R-project.org/>>.
- 1039 Rawding, D. J., Sharpe, C. S., & Blankenship, S. M. (2014). Genetic-Based Estimates of Adult
1040 Chinook Salmon Spawner Abundance from Carcass Surveys and Juvenile Out-Migrant
1041 Traps. *Transactions of the American Fisheries Society*, 143(1), 55–67.
1042 <https://doi.org/10.1080/00028487.2013.829122>
- 1043 Reed, T. E., Schindler, D. E., Hague, M. J., Patterson, D. A., Meir, E., Waples, R. S., & Hinch,
1044 S. G. (2011). Time to Evolve? Potential Evolutionary Responses of Fraser River Sockeye
1045 Salmon to Climate Change and Effects on Persistence. *PLoS ONE*, 6(6), e20380.
1046 <https://doi.org/10.1371/journal.pone.0020380>
- 1047 Reynolds, J. H., Woody, C. A., Gove, N. E., & Fair, L. F. (2007). Efficiently Estimating Salmon
1048 Escapement Uncertainty Using Systematically Sampled Data. *American Fisheries*
1049 *Society*, 54.
- 1050 Richards, P., Williams, J., Power, S. J. H., Boyce, I., & Foos, A. (2017). Migration, Tagging
1051 Response, and Distribution of Chinook Salmon Returning to the Taku River, 2018.
1052 *Alaska Department of Fish and Game, Division of Sport Fish, Regional Operational Plan*
1053 *ROP.SF.1J.2018.06, Anchorage.*

- 1054 Riddell, B.E., Howard, K.G., Munro, A.R. (2022). Salmon returns in the Northeast Pacific in
1055 relation to expedition observations (and next steps). *North Pacific Anadromous Fish*
1056 *Commission Technical Report 115-139*.
- 1057 Roff, D. A. (1973). On the Accuracy of Some Mark-Recapture Estimators. *Oecologia*, 12(1), 15–
1058 34. <https://doi.org/10.1007/BF00345468>
- 1059 Rousset, F. (2008). genepop’007: a complete re-implementation of the genepop software for
1060 Windows and Linux. *Molecular Ecology Resources*, 8, 103-106.
1061 <https://doi.org/10.1111/j.1471-8286.2007.01931.x>
- 1062 Sard, N. M., O’Malley, K. G., Jacobson, D. P., Hogansen, M. J., Johnson, M. A., & Banks, M.
1063 A. (2015). Factors Influencing Spawner Success in a Spring Chinook Salmon
1064 (*Oncorhynchus tshawytscha*) Reintroduction Program. *Canadian Journal of Fisheries*
1065 *and Aquatic Sciences*, 72(9), 1390–1397. <https://doi.org/10.1139/cjfas-2015-0007>
- 1066 Seber, G. A. F. (1982). *The Estimation of Animal Abundance and Related Parameters*.
- 1067 Seber, G. A. F., & Felton, R. (1981). *Tag Loss and the Petersen Mark-Recapture Experiment*.
1068 10.
- 1069 Seeb, L., Antonovich, A., Banks, M., Beacham, T., Bellinger, M., Blankenship, S., Campbell,
1070 M., Decovich, N., Garza, J., Guthrie, C., & Lundrigan, T. (2007). Development of
1071 Standardized DNA Database for Chinook Salmon. *Fisheries*.
- 1072 Sethi, S. A., & Tanner, T. (2014). Spawning distribution and abundance of a northern Chinook
1073 salmon population. *Fisheries Management and Ecology*, 21(6), 427–438.
1074 <https://doi.org/10.1111/fme.12091>

- 1075 Shedd, K., & Gilk-Baumer, S. (2021). *Chinook Salmon Genetic Baseline Update for Southeast*
1076 *Alaska and Canadian AABM fisheries* (Final Report NF-2019-I-10A; PSC Northern
1077 Fund). Alaska Department of Fish and Game - Gene Conservation Laboratory.
- 1078 Shedd, K. R., Lescak, E. A., Habicht, C., Knudsen, E. E., Dann, T. H., Hoyt, H. A., Prince, D. J.,
1079 & Templin, W. D. (2022). Reduced Relative Fitness in Hatchery-Origin Pink Salmon in
1080 Two Streams in Prince William Sound, Alaska. *Evolutionary Applications*, *15*(3), 429–
1081 446. <https://doi.org/10.1111/eva.13356>
- 1082 Small, M. P., Scofield, C., Griffith, J., Spidle, A., Verhey, P., & Bowman, C. (2020). *2018*
1083 *Broodyear Report: Abundance estimates for Stillaguamish River Chinook Salmon Using*
1084 *Trans-Generational Genetic Mark Recapture*. 44.
- 1085 Wacker, S., Skaug, H. J., Forseth, T., Solem, Ø., Ulvan, E. M., Fiske, P., & Karlsson, S. (2021).
1086 Considering Sampling Bias in Close-Kin Mark–Recapture Abundance Estimates of
1087 Atlantic Salmon. *Ecology and Evolution*, *11*(9), 3917–3932.
1088 <https://doi.org/10.1002/ece3.7279>
- 1089 Wang, J., & Santure, A. W. (2009). Parentage and Sibship Inference From Multilocus Genotype
1090 Data Under Polygamy. *Genetics*, *181*(4), 1579–1594.
1091 <https://doi.org/10.1534/genetics.108.100214>
- 1092 Waples, R. S. (2022). *TheWeight* : A Simple and Flexible Algorithm for Simulating Non-Ideal,
1093 Age-Structured Populations. *Methods in Ecology and Evolution*, *13*(9), 2030–2041.
1094 <https://doi.org/10.1111/2041-210X.13926>
- 1095 Waples, R. S., & Feutry, P. (2022). Close-Kin Methods to Estimate Census Size and Effective
1096 Population Size. *Fish and Fisheries*, *23*(2), 273–293. <https://doi.org/10.1111/faf.12615>

- 1097 Whitmore, R. W. (2016). Evaluation of Parameter Estimation and Field Application of
 1098 Transgenerational Genetic Mark-Recapture. Humboldt State University.
- 1099 Wingfield, J. C., & Sapolsky, R. M. (2003). Reproduction and Resistance to Stress: When and
 1100 How. *Journal of Neuroendocrinology*, *15*(8), 711–724. [https://doi.org/10.1046/j.1365-](https://doi.org/10.1046/j.1365-2826.2003.01033.x)
 1101 [2826.2003.01033.x](https://doi.org/10.1046/j.1365-2826.2003.01033.x)
- 1102 Yeakel, J. D., Gibert, J. P., Gross, T., Westley, P. A. H., & Moore, J. W. (2018). Eco-
 1103 evolutionary dynamics, density-dependent dispersal and collective behaviour:
 1104 Implications for salmon metapopulation robustness. *Philosophical Transactions of the*
 1105 *Royal Society B: Biological Sciences*, *373*(1746), 20170018.
 1106 <https://doi.org/10.1098/rstb.2017.0018>
- 1107 Zhou, S. (2002). Size-Dependent Recovery of Chinook Salmon in Carcass Surveys. *Transactions*
 1108 *of the American Fisheries Society*, *9*.

1109 Appendix

1110 Appendix S1: Single nucleotide polymorphism and microsatellite loci used to genotype Chilkat
 1111 River Chinook salmon.

Locus	Source
ARNT	Hess et al., 2014
GTH2B-550	Hess et al., 2014
NOD1	Hess et al., 2014
Ots_100884-287	Hess et al., 2014
Ots_101119-381	Hess et al., 2014
Ots_101554-407	Hess et al., 2014
Ots_101704-143	Hess et al., 2014
Ots_101770-82	Hess et al., 2014
Ots_102213-210	Hess et al., 2014
Ots_102414-395	Hess et al., 2014
Ots_102457-132	Hess et al., 2014
Ots_102801-308	Hess et al., 2014
Ots_102867-609	Hess et al., 2014
Ots_103041-52	Hess et al., 2014

Ots_103122-180	Hess et al., 2014
Ots_104048-194	Hess et al., 2014
Ots_104415-88	Hess et al., 2014
Ots_105105-613	Hess et al., 2014
Ots_105132-200	Hess et al., 2014
Ots_105385-421	Hess et al., 2014
Ots_105401-325	Hess et al., 2014
Ots_105407-117	Hess et al., 2014
Ots_105897-124	Hess et al., 2014
Ots_106313-729	Hess et al., 2014
Ots_106499-70	Hess et al., 2014
Ots_106747-239	Hess et al., 2014
Ots_107074-284	Hess et al., 2014
Ots_107285-93	Hess et al., 2014
Ots_107607-315	Hess et al., 2014
Ots_107806-821	Hess et al., 2014
Ots_108007-208	Hess et al., 2014
Ots_108390-329	Hess et al., 2014
Ots_108735-302	Hess et al., 2014
Ots_108820-336	Hess et al., 2014
Ots_109525-816	Hess et al., 2014
Ots_109693-392	Hess et al., 2014
Ots_110064-383	Hess et al., 2014
Ots_110201-363	Hess et al., 2014
Ots_110381-164	Hess et al., 2014
Ots_110551-64	Hess et al., 2014
Ots_110689-218	Hess et al., 2014
Ots_111084b-619	Hess et al., 2014
Ots_111312-435	Hess et al., 2014
Ots_111681-657	Hess et al., 2014
Ots_112208-722	Hess et al., 2014
Ots_112301-43	Hess et al., 2014
Ots_112419-131	Hess et al., 2014
Ots_112876-371	Hess et al., 2014
Ots_113242-216	Hess et al., 2014
Ots_113457-40R	Hess et al., 2014
Ots_115987-325	Hess et al., 2014
Ots_117242-136	Hess et al., 2014
Ots_117259-271	Hess et al., 2014
Ots_117370-471	Hess et al., 2014
Ots_117432-409	Hess et al., 2014
Ots_118175-479	Hess et al., 2014

Ots_118205-61	Hess et al., 2014
Ots_118938-325	Hess et al., 2014
Ots_120950-417	Hess et al., 2014
Ots_122414-56	Hess et al., 2014
Ots_123048-521	Hess et al., 2014
Ots_123921-111	Hess et al., 2014
Ots_124774-477	Hess et al., 2014
Ots_127236-62	Hess et al., 2014
Ots_127760-569	Hess et al., 2014
Ots_128302-57	Hess et al., 2014
Ots_128693-461	Hess et al., 2014
Ots_128757-61R	Hess et al., 2014
Ots_129144-472	Hess et al., 2014
Ots_129170-683	Hess et al., 2014
Ots_129458-451	Hess et al., 2014
Ots_129870-55	Hess et al., 2014
Ots_130720-99	Hess et al., 2014
Ots_131460-584	Hess et al., 2014
Ots_131802-393	Hess et al., 2014
Ots_131906-141	Hess et al., 2014
Ots_2KER-137	Hess et al., 2014
Ots_94857-232R	Hess et al., 2014
Ots_94903-99R	Hess et al., 2014
Ots_96222-525	Hess et al., 2014
Ots_96500-180	Hess et al., 2014
Ots_96899-357R	Hess et al., 2014
Ots_97077-179R	Hess et al., 2014
Ots_97660-56	Hess et al., 2014
Ots_98409-850	Hess et al., 2014
Ots_98683-796	Hess et al., 2014
Ots_99550-204	Hess et al., 2014
Ots_aldb-177M	Hess et al., 2014
Ots_AldB1-122	Hess et al., 2014
Ots_AldoB4-183	Hess et al., 2014
Ots_arp-436	Hess et al., 2014
Ots_AsnRS-72	Hess et al., 2014
Ots_aspat-196	Hess et al., 2014
Ots_CCR7	Hess et al., 2014
Ots_CD59-2	Hess et al., 2014
Ots_CD63	Hess et al., 2014
Ots_cgo24-22	Hess et al., 2014
Ots_Chin30up-211	Hess et al., 2014

Ots_CirpA	Hess et al., 2014
Ots_cox1-241	Hess et al., 2014
Ots_CRB211	Hess et al., 2014
Ots_crRAD10447-25	Hess et al., 2014
Ots_crRAD11620-55	Hess et al., 2014
Ots_crRAD12037-39	Hess et al., 2014
Ots_crRAD12711-37	Hess et al., 2014
Ots_crRAD13725-51	Hess et al., 2014
Ots_crRAD16540-50	Hess et al., 2014
Ots_crRAD17527-58	Hess et al., 2014
Ots_crRAD18289-33	Hess et al., 2014
Ots_crRAD18492-65	Hess et al., 2014
Ots_crRAD18937-60	Hess et al., 2014
Ots_crRAD20262-46	Hess et al., 2014
Ots_crRAD20376-66	Hess et al., 2014
Ots_crRAD20887-70	Hess et al., 2014
Ots_crRAD21115-24	Hess et al., 2014
Ots_crRAD22960-32	Hess et al., 2014
Ots_crRAD23631-48	Hess et al., 2014
Ots_crRAD25367-50	Hess et al., 2014
Ots_crRAD255-59	Hess et al., 2014
Ots_crRAD26081-28	Hess et al., 2014
Ots_crRAD26165-69	Hess et al., 2014
Ots_crRAD27164-55	Hess et al., 2014
Ots_crRAD27515-69	Hess et al., 2014
Ots_crRAD2806-42	Hess et al., 2014
Ots_crRAD28677-65	Hess et al., 2014
Ots_crRAD292-21	Hess et al., 2014
Ots_crRAD33054-62	Hess et al., 2014
Ots_crRAD33491-71	Hess et al., 2014
Ots_crRAD34397-33	Hess et al., 2014
Ots_crRAD35313-66	Hess et al., 2014
Ots_crRAD36072-29	Hess et al., 2014
Ots_crRAD36152-44	Hess et al., 2014
Ots_crRAD38095-29	Hess et al., 2014
Ots_crRAD38746-36	Hess et al., 2014
Ots_crRAD42058-48	Hess et al., 2014
Ots_crRAD44588-67	Hess et al., 2014
Ots_crRAD46081-56	Hess et al., 2014
Ots_crRAD46751-42	Hess et al., 2014
Ots_crRAD47297-55	Hess et al., 2014
Ots_crRAD5061-27	Hess et al., 2014

Ots_crRAD55400-59	Hess et al., 2014
Ots_crRAD55475-26	Hess et al., 2014
Ots_crRAD57376-68	Hess et al., 2014
Ots_crRAD57520-66	Hess et al., 2014
Ots_crRAD57687-34	Hess et al., 2014
Ots_crRAD60614-46	Hess et al., 2014
Ots_crRAD60620-51	Hess et al., 2014
Ots_crRAD61523-71	Hess et al., 2014
Ots_crRAD66330-60	Hess et al., 2014
Ots_crRAD69327-53	Hess et al., 2014
Ots_crRAD73823-60	Hess et al., 2014
Ots_crRAD74766-28	Hess et al., 2014
Ots_crRAD75581-70	Hess et al., 2014
Ots_crRAD78968-46	Hess et al., 2014
Ots_crRAD92420-25	Hess et al., 2014
Ots_crRAD9615-69	Hess et al., 2014
Ots_DDX5-171	Hess et al., 2014
Ots_EndoRB1-486	Hess et al., 2014
Ots_EP-529	Hess et al., 2014
Ots_Est1363	Hess et al., 2014
Ots_Est740	Hess et al., 2014
Ots_ETIF1A	Hess et al., 2014
Ots_FARSLA-220	Hess et al., 2014
Ots_FGF6A	Hess et al., 2014
Ots_FGF6B	Hess et al., 2014
Ots_GCSH	Hess et al., 2014
Ots_GDH-81x	Hess et al., 2014
Ots_GH2	Hess et al., 2014
Ots_GNRH2-278	Hess et al., 2014
Ots_GPDH	Hess et al., 2014
Ots_GPH-318	Hess et al., 2014
Ots_GST-207	Hess et al., 2014
Ots_GST-375	Hess et al., 2014
Ots_HFABP-34	Hess et al., 2014
Ots_HMGB1-73	Hess et al., 2014
Ots_hnRNPL-533	Hess et al., 2014
Ots_hsc71-3prime-488	Hess et al., 2014
Ots_hsc71-5prime-453	Hess et al., 2014
Ots_hsp27b-150	Hess et al., 2014
Ots_Hsp90a	Hess et al., 2014
Ots_HSP90B-100	Hess et al., 2014
Ots_IGF1-91	Hess et al., 2014

Ots_IK1-328	Hess et al., 2014
Ots_IL11	Hess et al., 2014
Ots_IsoT	Hess et al., 2014
Ots_LEI-292	Hess et al., 2014
Ots_mapK-3prime-309	Hess et al., 2014
Ots_mapKpr-151	Hess et al., 2014
Ots_MetA	Hess et al., 2014
Ots_mybp-85	Hess et al., 2014
Ots_Myc-366	Hess et al., 2014
Ots_myo1a-384	Hess et al., 2014
Ots_myoD-364	Hess et al., 2014
Ots_nelfd-163	Hess et al., 2014
Ots_NFYB-147	Hess et al., 2014
Ots_nkef-192	Hess et al., 2014
Ots_nramp-321	Hess et al., 2014
Ots_ntl-255	Hess et al., 2014
Ots_OPLW-173	Hess et al., 2014
Ots_OPSW-152	Hess et al., 2014
Ots_Ostm1	Hess et al., 2014
Ots_OTALDBINT1-SNP1	Hess et al., 2014
Ots_OTNAML12_1-SNP1	Hess et al., 2014
Ots_Ots311-101x	Hess et al., 2014
Ots_OTSBMP-2-SNP1	Hess et al., 2014
Ots_OTSMTA-SNP1	Hess et al., 2014
Ots_OTSTF1-SNP1	Hess et al., 2014
Ots_P450	Hess et al., 2014
Ots_P450-288	Hess et al., 2014
Ots_P53	Hess et al., 2014
Ots_parp3-286	Hess et al., 2014
Ots_PEMT	Hess et al., 2014
Ots_pigh-105	Hess et al., 2014
Ots_pop5-96	Hess et al., 2014
Ots_ppie-245	Hess et al., 2014
Ots_Prl2	Hess et al., 2014
Ots_RAD1104-38	Hess et al., 2014
Ots_RAD1832-39	Hess et al., 2014
Ots_RAD3513-49	Hess et al., 2014
Ots_RAD7936-50	Hess et al., 2014
Ots_RAD9480-51	Hess et al., 2014
Ots_RAS1	Hess et al., 2014
Ots_redd1-187	Hess et al., 2014
Ots_RFC2	Hess et al., 2014

Ots_SClkF2	Hess et al., 2014
Ots_SERPC1-209	Hess et al., 2014
Ots_SL	Hess et al., 2014
Ots_slc7a2-71	Hess et al., 2014
Ots_stk6-516	Hess et al., 2014
Ots_TAPBP	Hess et al., 2014
Ots_TCTA-58	Hess et al., 2014
Ots_TGFB	Hess et al., 2014
Ots_Thio	Hess et al., 2014
Ots_TLR3	Hess et al., 2014
Ots_TNF	Hess et al., 2014
Ots_Tnsf	Hess et al., 2014
Ots_tpx2-125	Hess et al., 2014
Ots_trnau1ap-86	Hess et al., 2014
Ots_txnip-321	Hess et al., 2014
Ots_u07-07.161	Hess et al., 2014
Ots_u07-17.135	Hess et al., 2014
Ots_u07-17.373	Hess et al., 2014
Ots_u07-18.378	Hess et al., 2014
Ots_u07-19.260	Hess et al., 2014
Ots_u07-20.332	Hess et al., 2014
Ots_u07-25.325	Hess et al., 2014
Ots_u07-49.290	Hess et al., 2014
Ots_u07-53.133	Hess et al., 2014
Ots_u07-57.120	Hess et al., 2014
Ots_u07-64.221	Hess et al., 2014
Ots_u1002-75	Hess et al., 2014
Ots_u1004-117	Hess et al., 2014
Ots_u1006-171	Hess et al., 2014
Ots_u1007-124	Hess et al., 2014
Ots_u1008-108	Hess et al., 2014
Ots_U211	Hess et al., 2014
Ots_U2362-227	Hess et al., 2014
Ots_U2362-330	Hess et al., 2014
Ots_U2446-123	Hess et al., 2014
Ots_U2567-104	Hess et al., 2014
Ots_U5049-250	Hess et al., 2014
Ots_U5121-34	Hess et al., 2014
Ots_UNKN4-150	Hess et al., 2014
Ots_UNKN6-187	Hess et al., 2014
Ots_USMG5-67	Hess et al., 2014
Ots_vatf-251	Hess et al., 2014

Ots_zn593-346	Hess et al., 2014
Ots_zP3b	Hess et al., 2014
Ots_ZR-575	Hess et al., 2014
PGK-54	Hess et al., 2014
RAG3	Hess et al., 2014
S7-1	Hess et al., 2014
unkn526	Hess et al., 2014
Omm1080	Seeb et al., 2007; Moran et al., 2013
Ots201b	Seeb et al., 2007; Moran et al., 2013
Ots213	Seeb et al., 2007; Moran et al., 2013
Ots9	Seeb et al., 2007; Moran et al., 2013
Ssa408uos	Seeb et al., 2007; Moran et al., 2013

1112